



UNICA

UNIVERSITÀ  
DEGLI STUDI  
DI CAGLIARI



Università di Cagliari

UNICA IRIS Institutional Research Information System

**This is the Author's [*accepted*] manuscript version of the following contribution:**

De Luca MA, Tocco G, Mostallino R, Laus A, Caria F, Musa A, Pintori N, Ucha M, Poza C, Ambrosio E, Di Chiara G, Castelli MP. Pharmacological characterization of novel synthetic opioids: Isotonitazene, metonitazene, and piperidylthiambutene as potent  $\mu$ -opioid receptor agonists. *Neuropharmacology*. 2022 Dec 15;221:109263.

**The publisher's version is available at:**

[http://dx.doi.org/\[doi: 10.1016/j.neuropharm.2022.109263.\]](http://dx.doi.org/[doi: 10.1016/j.neuropharm.2022.109263.])

]

**When citing, please refer to the published version.**

**PHARMACOLOGICAL CHARACTERIZATION OF NOVEL SYNTHETIC OPIOIDS:  
ISOTONITAZENE, METONITAZENE, AND PIPERIDYLTHIAMBUTENE AS POTENT  
MU OPIOID RECEPTOR AGONISTS**

**Maria Antonietta De Luca<sup>1</sup>, Graziella Tocco<sup>2</sup>, Rafaela Mostallino<sup>1</sup>, Antonio Laus<sup>2</sup>, Francesca Caria<sup>1</sup>, Aurora Musa<sup>1</sup>, Nicholas Pintori<sup>1</sup>, Marcos Ucha<sup>3</sup>, Celia Poza<sup>3</sup>, Emilio Ambrosio<sup>3</sup>, Gaetano Di Chiara<sup>1,4</sup>, and M. Paola Castelli<sup>1</sup>**

<sup>1</sup> *Department of Biomedical Sciences, University of Cagliari*

<sup>2</sup> *Department of Life and Environmental Sciences, University of Cagliari*

<sup>3</sup> *Department of Psychobiology, National University for Distance Learning (UNED), Madrid, Spain.*

<sup>4</sup> *CNR Institute of Neuroscience, Cagliari Section, University of Cagliari, Italy*

Running title: Nitazenes pharmacology

Correspondence to: [dichiara@unica.it](mailto:dichiara@unica.it) & [castelli@unica.it](mailto:castelli@unica.it)

Gaetano Di Chiara & Maria Paola Castelli

Department of Biomedical Sciences

University of Cagliari (Italy)

Phone: +390706754065

[mail: castelli@unica.it](mailto:castelli@unica.it), [dichiara@unica.it](mailto:dichiara@unica.it)

## **ABBREVIATIONS**

ACN, acetonitrile;

BPMD, binding pose metadynamics;

BRS, behavioral rating scale;

BSA, bovine serum albumin;

CHO, Chinese hamster ovary;

CNS, central nervous system;

CV, collective variables;

DA, dopamine;

DAMGO, [D-Ala<sup>2</sup>, NMe-Phe<sup>4</sup>, Gly-ol<sup>5</sup>]-enkephalin;

DMSO, dimethyl sulfoxide;

EDTA, ethylenediaminetetraacetic acid;

E<sub>max</sub>, maximal efficacy;

FCS, fetal calf serum;

GDP, Guanosine 5'-diphosphate;

[<sup>35</sup>S]GTPγS, guanosine 5'-(γ-thio)triphosphate;

Glide/XP, extra Precision Glide Score;

GTPγS, guanosine 5'-O-(3-thiotriphosphate);

IFD, induced fit docking;

ITZ, isotanitazene;

MM-GBSA, molecular mechanics generalized Born surface area;

MD, molecular dynamics;

MTD, metadynamic simulations;

MOR, μ opioid receptor;

MTZ, metonitazene;

NAL, naloxone;

NSOs, Novel Synthetic Opioids;

PBS, phosphate buffered saline;

PTB, piperidylthiambutene;

RM, repeated measures;

RMSD, root-mean-square deviation;

## Abstract

Recent trends of opioid abuse and related fatalities have highlighted the critical role of Novel Synthetic Opioids (NSOs). We studied the  $\mu$ -opioid-like properties of isotonitazene (ITZ), metonitazene (MTZ), and piperidylthiambutene (PTB) using different approaches. *In vitro* studies showed that ITZ and MTZ displayed a higher potency in both rat membrane homogenates ( $EC_{50}$ : 0.99 and 19.1 nM, respectively) and CHO-MOR ( $EC_{50}$ : 0.71 and 10.0 nM, respectively) than [D-Ala<sup>2</sup>, NMe-Phe<sup>4</sup>, Gly-ol<sup>5</sup>]-enkephalin (DAMGO), with no difference in maximal efficacy ( $E_{max}$ ) between DAMGO and NSOs. ITZ also has higher affinity ( $K_i$ : 0.06 and 0.05 nM) at the MOR than DAMGO in both systems, whilst MTZ has higher affinity in CHO-MOR ( $K_i$ =0.23 nM) and similar affinity in rat cerebral cortex ( $K_i$ =0.22 nM). PTB showed lower affinity and potency than DAMGO. *In vivo*, ITZ displayed higher analgesic potency than fentanyl and morphine ( $ED_{50}$ : 0.00156, 0.00578, 2.35 mg/kg iv, respectively); ITZ (0.01 mg/kg iv) and MTZ (0.03 mg/kg iv) reduced behavioral activity and increased dialysate dopamine (DA) in the NAc shell (max. about 200% and 170% over basal value, respectively). Notably, ITZ elicited an increase in DA comparable to that of higher dose of morphine (1 mg/kg iv), but higher than the same dose of fentanyl (0.01 mg/kg iv). *In silico*, induced fit docking (IFD) and metadynamic simulations (MTD) showed that binding modes and structural changes at the receptor, ligand stability, and the overall energy score of NSOs were consistent with the results of the biological assays.

**Keywords:** GTP $\gamma$ S binding; MOR binding; in silico studies; dopamine; nitazenes; nociception; microdialysis

## 1. Introduction

Since 2016, the United States have been stricken by an epidemic of opioid-related deaths (Bauman and Pasternak, 2018), initiated by opioid analgesic prescription, such as hydrocodone and oxycodone, and driven by fentanyl and novel synthetic opioids (NSOs) (<https://www.cdc.gov/nchs/nvss/vsrr/drug-overdose-data.htm>) (Prekupec et al., 2017). In Europe, opioid use and related deaths have not reached the epidemic dimensions of North America (European Drug Report, 2021); nevertheless, the European Monitoring Centre for Drugs and Drug Addiction (EMCDDA) regards NSOs as a serious threat and has accordingly implemented a series of actions aimed at assessing the risks inherent to their diffusion (De Luca and Di Chiara, 2019; Seyler et al., 2021) ([https://www.emcdda.europa.eu/spotlights/fentanils-and-other-new-opioids\\_en](https://www.emcdda.europa.eu/spotlights/fentanils-and-other-new-opioids_en)). In this context, preclinical pharmacological studies are of utmost importance in order to characterize the biological effects of NSOs (Baumann et al., 2018; Baumann and Pasternak, 2018).

Besides fentanyl and its analogues, various non-fentanyl-related NSOs, such as cyclohexylphenols (e.g., *O*-desmethyltramadol), cyclohexylbenzamides (e.g., U-47700, AH-7921), diphenethylpiperazines (e.g., MT-45), cinnamylpiperazines (e.g., 2-methyl-AP-237), thiambutenes (e.g., Piperidylthiambutene [PTB]), and 2-benzylbenzimidazole derivatives (e.g., etonitazene, metonitazene [MTZ], clonitazene) have been introduced in the illicit drug market (Prekupec et al., 2017; Ujváry et al., 2021; Vandeputte et al., 2021a). Etonitazene analogs, also referred to as “nitazenes”, were developed in the mid-1950s by the pharmaceutical company CIBA (Hunger et al., 1960; Rossi et al., 1960) in the search for better and safer opioid analgesics (Gross and Turrian, 1957; Hoffmann et al., 1960). Several benzimidazole derivatives displayed a higher antinociceptive effect in mice than morphine, with etonitazene being the most potent derivative (Gross and Turrian, 1957; Hunger et al., 1960a,b).

Isotonitazene (ITZ), the second most potent benzimidazole analogue synthesized and patented in 1959 by CIBA, is an analgesic 500 times more potent than morphine in mice (Hunger et al., 1960a,b; Ujváry et al., 2021). In the NSO market, ITZ was firstly identified in August 2019 and remained

dominant until the first half of 2020 (Blanckaert et al., 2020; Vandeputte et al., 2021b), when it was temporarily included in Schedule I (June 2020) and definitively internationally scheduled in June 2021 (UNODC, 2021). ITZ has been detected in biological samples from fatalities in the USA, Canada and in the European Union (EMCDDA, 2020; World Health Organization, 2020; Shover et al., 2021; Mueller et al. 2021; Logan et al., 2020).

Using an *in vitro* live cell-based reporter assay, two recent studies (Blanckaert et al., 2020; Vandeputte et al., 2021a) showed that ITZ displays a higher potency and efficacy than hydromorphone at the  $\mu$ -opioid receptor (MOR). Moreover, when ITZ was evaluated in a guanosine 5'-( $\gamma$ -thio)triphosphate ( $[^{35}\text{S}]\text{GTP}\gamma\text{S}$ ) functional assay using preparations of transfected CHO cells expressing human  $\delta$ - or  $\kappa$ - opioid receptors or rat MORs, it fully stimulated all these receptors, displaying the highest potency and efficacy at the MOR than at the  $\delta$ - or  $\kappa$ - receptor. Additionally, in CHO-MOR, ITZ was more potent than  $[\text{D-Ala}^2, \text{NMe-Phe}^4, \text{Gly-ol}^5]\text{-enkephalin}$  (DAMGO) and fentanyl in activating  $[^{35}\text{S}]\text{GTP}\gamma\text{S}$  binding (US Drug Enforcement Administration-Veterans Affairs (DEA-VA) Interagency Agreement 2019). Although ITZ has never been studied in clinical trials, the available pharmacological information and the similarity with other opioid analgesics suggest that the most serious acute risk from the use of ITZ in humans seems to be respiratory depression, which can lead to apnea, respiratory arrest, and death (EMCDDA, 2020).

Regarding dosages and routes of administration, the only information available is from forensic reports (Krotulski et al., 2020) and online forums (e.g., bluelight.org; drugs-forum.com). In humans, intravenous, sublingual, or inhalation dosages are between 1 and 10 mg/kg and 100 and 200  $\mu\text{g}/\text{kg}$  by nasal spray. A forensic study by Krotulski et al. (2020) reported that ITZ concentrations in biological specimens were at sub-**to nanogram/milliliter concentrations** (e.g., the average concentration was  $2.2 \pm 2.1$  ng/mL and  $2.4 \pm 1.4$  ng/ml in blood and urine samples, respectively) underscoring the need for high sensitivity analytical methods.

Metonitazene (MTZ) is one of the newest non-fentanyl NSOs that has emerged in the illicit drug market followed by other analogues of nitazenes such as N-Piperidinyl etonitazene also termed

'etonitazepipne' (Vandeputte et al., 2022). MTZ was found in North Carolina (USA) in July 2020 (Krotulski et al., 2020) and in Germany in September 2020 (EU Early Warning System that has emerged [December 2020]) and was identified in 20 forensic post-mortem cases from several USA states (Tennessee, Illinois, Florida, Iowa, Ohio, South Carolina and Wisconsin) between January and February 2021. MTZ, bearing a 4-methoxyphenyl group instead of the 4-isopropoxyphenyl moiety of ITZ, is internationally scheduled since June 2022 (<https://www.unodc.org/LSS/Announcement/Details/a56e0bd9-0da5-4152-a34d-7cff7746bf50>).

Early preclinical studies reported that the antinociceptive relative potency of MTZ in mice is 100 times higher than that of 5 mg/kg morphine (Hunger et al., 1957, 1960a, 1960b). In preclinical studies performed in rodents, the analgesic potency of MTZ was estimated at 30-100 times more potent than morphine, depending on the administration route and the animal model used (Ujváry, et al., 2021). In morphine-addicted monkeys, MTZ was a hundred times more potent than morphine sulfate in suppressing physical abstinence but with a duration of action about half that of morphine (Deneau et al., 1959; Ujvary, 2020)

Together with clonitazene and etonitazene, MTZ was one of the few 2-benzylbenzimidazole studied in clinical trials as an analgesic in postoperative or injured patients in the late 1950s (Bromig, 1958). According to a clinical trial involving 363 patients, 1 mg/kg (subcutaneous or intramuscular) of MTZ produces analgesia often accompanied by sedation, drowsiness, vertigo, confusion, nausea, and vomiting (Ujváry et al., 2021). Respiratory depression with cyanosis was also observed in one-fifth of the patients and respiratory failure and coma in one patient. Recently, Krotulski et al. (2021) reported the presence of MTZ in combination with fentanyl, benzodiazepines, hallucinogens, and opioids in 20 forensic post-mortem cases. Finally, in  $\beta$ -arrestin2 and mini-Gi MOR activation assays, MTZ displayed a similar or slightly higher potency than fentanyl (Vandeputte et al., 2021a).

PTB has been illicitly marketed since 2018 and was first sold as a designer drug. It is an opioid with analgesic properties belonging to the thiambutene family, with a potency similar to that of morphine (Adamson et al., 1951; Green 1953). Like nitazenes, PTB's analgesic and antitussive properties were



reported in the 1950s (Adamson and Green, 1950; Green, 1953; Kase et al., 1955; Kimura et al., 1958) but the drug **was never tested in clinical studies**. Up to now, only one study has investigated the *in vitro* biological activity of PTB (Vandeputte et al., 2020) utilizing the same live cell-based assay for ITZ and MTZ and reporting that the potency of PTB at MOR is in the nanomolar range and associated with a high intrinsic activity. The information about the abuse liability of PTB and its structural analogues is limited. Recently, Arilotta et al. (2020) using the web crawler tool NPS Finder<sup>®</sup> identified PTB among 136 non-fentanyl analogues. Despite the widespread and growing use of NSOs, there is **a lack** of information about its rewarding and reinforcing properties. In particular, no preclinical studies have yet evaluated the effect of NSOs on dopamine (DA) transmission in the ventral striatal areas, such as the nucleus accumbens (NAc), considered a pivotal area in the central effects of narcotic analgesics and other classes of drugs of abuse (Di Chiara et al., 2004; Volkow et al., 2012).

The present experiments were designed to study the  $\mu$ -opioid-like properties of the NSOs ITZ, MTZ, and PTB (Fig. 1). Binding and agonistic properties of NSOs were investigated *in vitro* in both native (cortical rat brain homogenates) and recombinant systems expressing mouse MOR (CHO-MOR). *In vivo*, analgesic properties, effects on NAc shell DA transmission and on behavioral activity were also investigated and compared with those of the reference compounds (i.e., fentanyl and morphine). Moreover, ITZ, MTZ and PTB were investigated *in silico*. Induced Fit Docking (IFD) and Metadynamic simulations (MTD) experiments were performed to accurately predict the ligand binding modes and the concomitant structural changes in receptor and ligand stability.

## **2. Materials and Methods**

### *2.1. Animals*

Adult (weight 275-300 g) male Sprague-Dawley rats (Envigo, Italy or Charles River Laboratories [Lyon, France]) were employed for *in vitro* and *in vivo* experiments. Rats were housed in groups of

six in standard temperature ( $21 \pm 1^\circ\text{C}$ ) and humidity (60%) conditions under a 12h/12h light/dark cycle (lights on at 7.00 am) with food and water available *ad libitum*. All experiments were carried out in accordance with European Council directives (609/86 and 63/2010) and in compliance with the animal policies approved by the Italian Ministry of Health and the Ethical Committee for Animal Experiments (CESA, University of Cagliari, Italy), and the Bioethics Committee of the National University for Distance Learning (UNED, Madrid, Spain). We made all efforts to minimize pain and suffering and to reduce the number of animals used.

## 2.2. Drugs

Morphine hydrochloride, fentanyl hydrochloride, ITZ (N,N-diethyl-2-[[4-(1-methylethoxy)phenyl]methyl]-5-nitro-1H-benzimidazole-1-ethanamine), MTZ (N,N-diethyl-2-[[4-methoxyphenyl]methyl]-5-nitro-1H-benzimidazole-1-ethanamine), PTB (1-(1-methyl-3,3-di-2-thienyl-2-propen-1-yl)-piperidine, monohydrochloride), DAMGO, and naloxone (NAL) were purchased from Cayman Chemical Company (Michigan, USA). [ $^3\text{H}$ ]DAMGO, [Tyrosyl-3,5- $^3\text{H}$ (N)] and [ $^{35}\text{S}$ ]GTP $\gamma$ S (1250 Ci/mmol) were purchased from Perkin Elmer Life Sciences, Inc. (Boston, MA, USA). Guanosine 5'-diphosphate (GDP), and guanosine 5'-O-(3-thiotriphosphate) (GTP $\gamma$ S) were obtained from Sigma/RBI (St. Louis, MO, USA).

For biochemical experiments, all drugs except MTZ were dissolved in dimethyl sulfoxide (DMSO) and results are reported as free base for PTB, fentanyl and morphine. MTZ was dissolved in acetonitrile (ACN). The DMSO and ACN concentration used in the different assays never exceeded 0.1-0.2 % (v/v), respectively, and had no effects on [ $^3\text{H}$ ]DAMGO binding and [ $^{35}\text{S}$ ]GTP $\gamma$ S binding assays.

For behavioral experiments and *in vivo* microdialysis, drugs were solubilized (hydrochloride) or diluted (ACN solution) in saline and administered intravenously (i.v.; 1 ml/kg) at different dosages depending on the group of animals; morphine: 0.5-4 mg/kg; fentanyl: 0.00125-0.01 mg/kg; ITZ: 0.0005-0.01 mg/kg; MTZ: 0.001-0.03 mg/kg.

### 2.3. *In vitro* experiments

#### 2.3.1. *Cell culture*

CHO-MOR cells were kindly donated by Dr Pan (Memorial Sloan Kettering Cancer Center, New York, NY, USA). CHO-MOR cells were maintained in F-12 medium supplemented with 10% heat inactivated fetal calf serum (FCS) and grown at 37°C in a 5% CO<sub>2</sub> /95% air humidified atmosphere. Plates of cells were used when cell density reached 80–95% confluence, then cells were detached from the plate for the assay or for subculturing after incubation for 4 min at 37°C with ethylenediaminetetraacetic acid (EDTA) (1 mM) in phosphate-buffered saline (PBS).

#### 2.3.2. *Tissue and membrane preparation.*

*Rat cortical membrane preparation.* Rats were sacrificed by decapitation. Brains were collected and the whole brain minus cerebellum was used for the assay. For binding assays, tissues were homogenized in 50 volumes (w/v) of ice-cold 50 mM TRIS-HCl buffer (pH 7.4) using a Polytron homogenizer. The homogenate was centrifuged at 48.000g for 20 min at 4 °C, the supernatant was discarded, and the resulting pellet was resuspended in 50 volumes of fresh ice-cold buffer (pH 7.4) and incubated for 45 min at 37 °C in a water bath. Then, the homogenate was centrifuged again at 48.000g for 20 min at 4 °C. The resulting pellet was frozen at -80 °C for at least 18-20 h before use in the [<sup>3</sup>H]DAMGO binding assay. Aliquots of membranes were frozen at -80 °C until the day of the experiment.

For MOR-stimulated [<sup>35</sup>S]GTPγS binding, rat cortex was dissected and homogenized in a polytron with 20 volumes of buffer (50 mM Tris-HCl, 3 mM MgCl<sub>2</sub>, and 1 mM EGTA, pH 7.4). The homogenate was centrifuged at 48.000g at 4°C for 10 min, the supernatant discarded, and the pellet resuspended in a homogenization buffer, and centrifuged again at 48.000g for 10 min. The final pellet was resuspended in a GTPγS assay buffer and the aliquots frozen at -80 °C until use.

*CHO-MOR membrane preparation.* For the MOR binding assay, membranes from cells were prepared as previously described (Bolan et al., 2004). Briefly, membranes were harvested by manually detaching cells from their plates with a rubber septum into cold PBS. Then, cells were centrifuged at 1,200g for 10 min and the pellet was resuspended in 20 volumes of TRIS buffer (50 mM; pH 7.4 at 25°C), EDTA (1 mM), sodium chloride (100 mM), and phenylmethylsulfonylfluoride (10 µM). The homogenate was incubated at 25 °C for 15 min and centrifuged at 49.000g for 50 min. The resulting pellet was resuspended, and aliquots frozen at -80°C until use.

For MOR-stimulated [<sup>35</sup>S]GTPγS binding, CHO-MOR cells were harvested by replacing the medium with cold PBS containing 0.04% EDTA for 5 min, followed by agitation, and collected by centrifugation at 1.000g for 10 min. The pellet was resuspended in a GTPγS assay buffer and aliquots were frozen at -80 °C until use.

The Bradford (1976) protein assay was used for protein determination using bovine serum albumin (BSA) as a standard in accordance with supplier protocol (Bio- Rad, Milan, Italy).

### 2.3.3. [<sup>35</sup>S]GTPγS binding assay in rat cortical membranes and in CHO-MOR cell membranes

Membrane homogenates from rat cortical membranes (20 µg) or CHO-MOR (30-50 µg) were incubated for 60 min at 30°C with and without drugs, in a final volume of 1 ml assay buffer (50 mM Tris-HCl, 3 mM MgCl<sub>2</sub>, 0.2 mM EGTA, 100 mM NaCl, pH 7.4) containing 0.05 nM [<sup>35</sup>S]GTPγS and 30 µM or 10 µM GDP for rat cortical- and CHO-membranes, respectively. After incubation, samples were filtered using a Packard Unifilter- GF/B, washed twice with 1 ml of ice-cold 50 mM Tris-HCl, pH 7.4 buffer, and dried for 1 h at 30 °C. The radioactivity on the filters was counted in a liquid microplate scintillation counter (TopCount NXT, Packard, Meridien, CT) using 30 µl of scintillation fluid (Microscint 20, Packard, Meridien, CT). In rat cortical membranes DAMGO, ITZ, MTZ and PTB were incubated alone at a fixed concentration of 1 µM or in combination with the MOR antagonist, NAL (5 µM). Concentration-effect curves were determined by incubating rat cortical- or

CHO-MOR with various concentrations of compounds (ITZ, MTZ, fentanyl, PTB, DAMGO and ITZ, MTZ, DAMGO, PTB, respectively) (1 pM to 100  $\mu$ M) in the presence of 0.05 nM [ $^{35}$ S] GTP $\gamma$ S and 30  $\mu$ M or 10  $\mu$ M GDP for rat cortical- and CHO-MOR, respectively. Nonspecific binding was measured in the presence of 10  $\mu$ M unlabeled GTP $\gamma$ S. Basal binding was assayed in the absence of agonists//the agonist and in the presence of GDP. Stimulation by the agonist was defined as a percentage increase above basal levels (i.e., {[dpm(agonist)- dpm(no agonist)]/dpm(no agonist)} x100). Data are reported as the mean  $\pm$  SEM of three to four experiments, performed in triplicate. In line with previous studies (De Luca et al., 2016 Porcu et al., 2018), GraphPad Prism 8 software (San Diego, CA, U.S.) was used to subsequently generate concentration–response curves via three-parameter logistic regression to calculate Emax (maximal stimulation over basal levels) and EC<sub>50</sub> (agonist concentration needed to obtain 50% of the maximal effect) values.

#### 2.3.4. [ $^3$ H]DAMGO binding assay in brain and CHO-MOR cell membranes

Membrane homogenates from rat brain membranes (300-400  $\mu$ g) were incubated for 60 min at 25  $^{\circ}$ C with 1 nM of [ $^3$ H]DAMGO in a volume of 2 ml of 50 mM buffer TRIS-HCl, pH 7.4. Nonspecific binding was determined in the presence of 10  $\mu$ M NAL. [ $^3$ H]DAMGO binding for CHO-MOR was carried out as described by Bolan et al. (2004), with slight modifications. Briefly, aliquots of CHO-MOR membranes (40-50  $\mu$ g of protein), resuspended in 50 mM potassium phosphate buffer, pH 7.4, containing 5 mM magnesium sulfate, were incubated with [ $^3$ H]DAMGO (1 nM) at room temperature (25  $^{\circ}$ C) for 60 min in a final volume of 2 ml assay buffer. Nonspecific binding was determined using NAL (10  $\mu$ M). In both binding assays, free ligand was separated from bound ligand by rapid filtration through Whatman GF/B filters, using a Brandell 30-sample harvester (Gaithersburg, MD). Filters were washed three times with ice-cold Tris-HCl buffer (pH 7.4). Filter-bound radioactivity was counted in a liquid scintillation counter (Packard Tricarb 2810 TR, Packard, Meridien, CT), using 3 ml of scintillation fluid (Ultima Gold Packard, MV, Meridien, CT). [ $^3$ H]DAMGO displacement curves were carried out using serial dilutions ranging from  $10^{-12}$  to

$10^{-5}$  M of the unlabeled compounds (ITZ, MTZ, fentanyl, PTB, DAMGO in rat cortical membranes; ITZ, MTZ, PBT, DAMGO in CHO-MOR cell membranes, respectively) and [ $^3$ H]DAMGO (1 nM). Independent experiments were repeated on membrane preparations from at least three different experiments, performed in triplicate. The calculation of the IC<sub>50</sub> (the concentration that inhibits 50% of specific radioligand binding) was performed by nonlinear curve fitting of the concentration effect curves via three-parameter logistic regression using GraphPad Prism 8 software, San Diego, CA. The F-test was used to determine the best approximation of a nonlinear curve fit to a one- or two-site model ( $P < 0.05$ ). IC<sub>50</sub> values were converted to K<sub>i</sub> values by means of the Cheng and Prusoff equation (Cheng and Prusoff, 1973).

## *2.4 In vivo antinociception*

### *2.4.1 Intravenous catheterization for hot plate test*

Rats were administered with buprenorphine (0.05 mg/kg s.c.) in order to prevent early post-surgical pain. Later, they were placed in the pre-anesthetic chamber under 5% isoflurane gas (Forane, Abbott) and maintained under general anesthesia by 2% isoflurane during the surgical implant of a polyvinyl chloride catheter (0.064" i.d.) with a silicone end in the right jugular vein. Subsequently, the animals were allowed to recover for seven days. During the first five days, the rats were administered with meloxicam in their drinking water. One day before the start of the administration program, we checked the correct condition of the implanted catheter by infusing a sodium thiopental solution at a minimum dosage (10 mg/kg). If the animal showed immediate signs of loss of consciousness, the catheter was considered to be properly implanted. A further 0.4 ml of a saline solution composed of heparin (1.5 IU/ml) and gentamicin (40 mg/ml) was infused through the catheter daily to keep the catheter clean and functional and to prevent possible infections.

### *2.4.2 Hot plate test*

Nociception was studied in a hot plate test (Animal Research Analgesiometer, Model 35150, Ugo Basile) for laboratory rodents. More specifically, we performed **dose-response experiments** of hot

plate latency after ITZ (0.0005-0.004 mg/kg), fentanyl (0.00125-0.01 mg/kg), morphine (0.5-4 mg/kg) intravenous administration. Only ITZ was evaluated for its analgesic properties by the hot plate test because only ITZ induced a strong reduction in behavioral activity, as estimated by the behavioral rating score during microdialysis experiments. Indeed, MTZ displayed a mild and short time reduction in behavioral activity. In order to reduce the number of animals in the study, we therefore selected ITZ as the best candidate for the study on nociception.

Rats were placed on the plate surface at 52.5 °C and latency to hind paw licking or withdrawal response was measured by two different observers blind to treatment conditions. Rats were removed from the plate once the response was emitted or after 60 seconds to prevent tissue damage. Hind paw licking or withdrawal responses measured in the hot plate test are not present in spinally transected rats, so this test supposedly assesses supraspinal mediated antinociception (Deuis et al., 2017).

## *2.5 In vivo brain microdialysis*

### *2.5.1. Preparation of microdialysis probe*

Vertical microdialysis probes, with an active dialysing portion of 1 mm, were prepared with AN69 fibers (Hospal Dasco, Bologna, Italy) as previously described (De Luca et al., 2014).

### *2.5.2. Surgery for probe implant*

Male Sprague-Dawley rats (275-300 g; Harlan, Italy) were anesthetized with isoflurane gas (Merial, Milano, Italy) and maintained under anesthesia using a breathing tube under a scavenging system while placed in a stereotaxic apparatus and implanted with microdialysis probes in the NAc shell (A+2.2, L+1.0 from bregma, V-7.8 from dura) according to the rat brain atlas (Paxinos and Watson, 2007). In order to perform intravenous (i.v.) drug administration, a catheter (Silastic, Dow Corning Corporation, Michigan, USA) was inserted into the right jugular vein, as previously described (De Luca et al., 2014).

### 2.5.3. Analytical Procedure

On the day following surgery, probes were perfused with Ringer's solution (147 mM NaCl, 4 mM KCl, 2.2 mM CaCl<sub>2</sub>) at a constant rate of 1 µl/min. Dialysate samples (20 µl) were injected into an HPLC system equipped with a reverse phase column (C8 3.5 µm, Waters, USA) and a coulometric detector (ESA, Coulochem II) to quantify DA. The first electrode of the detector was set at +130 mV (oxidation) and the second at -175 mV (reduction). The composition of the mobile phase was: 50 mM NaH<sub>2</sub>PO<sub>4</sub>, 0.1 mM Na<sub>2</sub>-EDTA, 0.5 mM n-octyl sodium sulfate, 15% (v/v) methanol, pH 5.5. The sensitivity of the assay for DA was 5 fmol/sample. Dialysate DA from the NAc shell was evaluated in order to **perform dose-response experiments** after intravenous administration of ITZ (0.001-0.01 mg/kg) and MTZ (0.001-0.03 mg/kg) and to compare the extracellular levels of DA to those obtained after intravenous vehicle, morphine (1.0 mg/kg) or fentanyl (0.01 mg/kg).

### 2.5.4. Histology

At the end of the microdialysis experiment, the mice were deeply anesthetized and euthanized. The probes were removed and the brains stored in formalin (8%) for histological examination to verify the correct placement of the microdialysis probe. Brains were cut with a vibratome (Campden Instruments, Leics, UK) in serial coronal slices oriented according to Paxinos & Watson's mouse brain atlas (2007), and the location of the probes was reconstructed.

### 2.6 Behavioral evaluation

The Behavioral Rating Scale (BRS) used in the present study was adapted from Salamone et al. (1996) and consisted of a 6-point scale ranging from 0 to 5. The ratings were as follows: 0-asleep: eyes fully closed, body relaxed, asleep; 1-heavy sedation: eyes mostly closed, loss of righting reflex; 2-moderate sedation: head mostly or completely down, eyes partly closed, flattened posture, no spontaneous movement; 3-mild sedation: eyes partly closed, head somewhat down, impaired locomotion including abnormal posture, use of only some limbs, dragging and stumbling; 4-awake, inactive: eyes fully



open, head up, little to no locomotion, rearing or grooming, normal posture; 5-awake, active: engaged in locomotion, rearing, head movements or grooming. Measurements were scored by two different observers blind to treatment conditions. We evaluated the effect of nitazenes, morphine (1mg/kg), and the respective vehicle on sedation rating: three dosages of ITZ (0.001, 0.003, 0.01 mg/kg) and MTZ (0.001, 0.01, 0.03 mg/kg) were administered intravenously, and the rate of activity was compared with that observed after vehicle or morphine.

## 2.7 Statistical analysis

The results of *in vitro* studies are the mean of at least three or four independent experiments, performed in triplicate. Data are expressed as mean  $\pm$  SEM and differences were statistically significant at  $p < 0.05$ . Normality tests for data were carried out using the Shapiro-Wilk's test.

Statistical analysis for the [<sup>3</sup>H]DAMGO and [<sup>35</sup>S]GTP $\gamma$ S binding assay was performed using one-way ANOVA, followed by Dunnett's test for *post hoc* comparisons. Scatchard analysis of binding data was performed by a computer curve-fitting program (Ligand) for a single class of binding sites. The effect of treatment in the hot plate test, DA responses, and the time-course of the behavioral activity rate after morphine, fentanyl, ITZ, and MTZ challenges were analyzed by repeated measures (RM) two-way ANOVA (Treatment  $\times$  Time), followed by Tuckey's multiple comparison. For RM tests, whenever we could not assume sphericity, a Geisser-Greenhouse correction was carried out. The 10 min behavioral activity rate was analyzed by the non-parametric Kruskal Wallis test followed by Dunn's *post hoc* test. Statistical analysis was performed with GraphPad Prism 8 software (GraphPad Prism).

## 2.8 In silico studies

### 2.8.1 Construction of the Simulated Systems

The crystal structures of (*Mus musculus*) MOR in the active form bound to the BU72 agonist (PDB ID, 5C1M) and in the "inactive" form bound to the morphinan BF0 antagonist (PDB ID, 4DKL) were

obtained from the RCSB database at 2.07Å (5C1M) and 2.80Å (4DKL) RCSB-PDB. The structures were then prepared and refined by the protein preparation wizard tool (Maestro molecular modeling suite) (Huang et al., 2015; Manglik et al., 2012; Sastry et al., 2013). The Schrödinger Release 2021-1 (Schrödinger Release 2021-1: Maestro, Schrödinger, LLC, New York, NY) with the OPLS3e force field was used to prepare and dock the compounds into the receptors. Then, ITZ, MTZ, PTB and fentanyl were cross-docked into MOR binding sites before equilibration and the LigPrep module was used to build all compounds at pH 7.4. A net positive charge to each compound was assigned by Epik module before preparing the MOR model by the IFD protocol in the Schrödinger suite. A docking grid box was located no more than 5Å from the crystal ligand. Dockings were then performed using a standard protocol whereby conformations of the ligand were screened in the presence of an implicit membrane and solvent for clashes with the protein and subsequently refined by allowing flexibility of the sidechains in the binding (Harder et al., 2016; Greenwood et al., 2010; Sherman et al., 2006). A molecular method generalized-Born surface area (MM-GBSA) with default parameters and implicit membrane and solvent (Schrodinger Suite, Prime module) was used to calculate the free-binding energy of all complexes and to select the best poses for the binding pose Metadynamic simulations (Ylilauri and Pentikäinen, 2013). A binding pose MTD protocol was applied to study these docked models of MOR with all-atom MD simulations. All MTD simulations were carried out using GPUs and the Schrodinger suite Desmond tool. Binding Pose Metadynamics (BPMD), (Maestro version 12.5) were used to determine the ligand stability in solution (Fusani et al., 2020). BPMD experiments, averaged over 10 repeated independent MD simulations for 10 ns indicated collective variables (CV) as the measure of the root-mean-square deviation (RMSD) of the ligand heavy atoms relative to their starting position. Alignment prior to RMSD calculation was carried out by selecting protein residues within 3 Å of the ligand. Before calculating the heavy atom RMSD to the ligand conformation in the first frame, we aligned the Ca atoms of these binding site residues to those of the first frame of the MTD trajectory. The hill height and width were set to 0.05 kcal/mol (about 1/10 of the characteristic thermal energy of the system, kBT) and 0.02 Å, respectively. The

Metadynamics run was preceded by a system solvation in a box of SPC/E water molecules followed by several minimization and controlled molecular dynamics (MD) steps that allowed the system to gradually reach the desired temperature of 300 K as well as releasing any bad contacts and/or strain in the initial starting structure. The final snapshot of the short unbiased MD simulation of 0.5 ns was then used as the reference for the Metadynamics production phase.

### 3. Results

#### 3.1. *In vitro* studies

##### 3.1.1. Agonist-stimulated [<sup>35</sup>S]GTPγS and MOR binding to cortical rat membranes

At a concentration of 1 μM, the full agonist DAMGO (our reference compound) maximally stimulated GTPγS binding to rat cortex membranes by approximately  $30 \pm 3.9\%$  over basal activity. Fentanyl, ITZ, MTZ and PTB produced G-protein stimulation similar to DAMGO. The MOR antagonist NAL (5 μM) completely blocked GTPγS binding stimulated by DAMGO and by fentanyl, ITZ, MTZ and PTB, indicating that they produce G protein activation via MOR (Suppl. Fig.1). DAMGO and the other opioids stimulated [<sup>35</sup>S]GTPγS binding to rat cortex in a concentration-dependent and saturable manner (Fig. 2A and Table 1). ITZ, MTZ and fentanyl showed nanomolar potency at MOR, with ITZ, MTZ and fentanyl being 313-, 16- and 2.5-fold more potent than DAMGO, respectively (ANOVA:  $F_{(4,13)} = 65.00$ ,  $P < 0.0001$ ;  $p < 0.01$  Dunnett's post hoc test). On the contrary, PTB showed a lower potency than DAMGO in stimulating GTPγS binding (Table 1). No difference in the Emax of G-protein activation by DAMGO and other tested compounds was observed (ANOVA:  $F_{(4,13)} = 2.871$ ;  $P = 0.066$ ). Rank order of potency was ITZ > MTZ > fentanyl > DAMGO and > PTB (Table 1). In order to determine the MOR affinity of DAMGO and other compounds we performed a radiolabeled competitive binding assay in rat cortical membranes. According to previously published data (Yeadon and Kitchen 1988; Gillan and Kosterlitz 1982) the Kd and Bmax, obtained by Scatchard analysis of [<sup>3</sup>H]DAMGO saturation binding, were  $1.33 \pm 0.02$  nM and  $0.42 \pm$

0.04 pmol/mg protein, respectively (n=4, data not shown). As expected, DAMGO completely inhibited the specific binding of [<sup>3</sup>H]DAMGO with a K<sub>i</sub> of 0.23 ± 0.01 nM (Fig. 2B, Table 1). As shown in Figure 2B, fentanyl, MTZ, ITZ and PTB also displaced [<sup>3</sup>H]DAMGO binding in rat cortical membranes in a concentration dependent manner; K<sub>i</sub>'s ranged from 0.06 ± 0.01 nM for ITZ to 2.75 ± 0.03 nM for PTB (Table 1). Specifically, ITZ showed a 3.8-fold greater affinity than DAMGO, while MTZ displayed a similar affinity, and fentanyl and PTB showed a lower affinity than DAMGO. Thus, the rank order of the K<sub>i</sub> values of these compounds for MOR was ITZ < MTZ = DAMGO < fentanyl < PTB. **It is remarkable that, while DAMGO and MTZ show similar affinities for MOR, the potency of the latter is markedly higher.**

### 3.1.2. Agonist-stimulated [<sup>35</sup>S]GTPγS and MOR binding to CHO-MOR cell membranes

Next, we examined the effects of ITZ, MTZ, PTB, and DAMGO in radioligand binding and GTPγS functional assays in CHO-MOR (Bolan et al., 2004). As shown in Figures 3A and 3B, all NSO compounds stimulated [<sup>35</sup>S]GTPγS or inhibited [<sup>3</sup>H]DAMGO binding in a concentration-dependent manner. The Synoptic Table 2 shows the results of tested compounds for the displacement of [<sup>3</sup>H]DAMGO binding and their effects on GTPγS stimulation in a concentration-dependent manner in CHO-MOR. All NSOs displayed efficacies similar to DAMGO, acting as full agonists (Table 2). Consistent with the [<sup>35</sup>S]GTPγS binding data, ITZ and MTZ have respectively 24 and 5 times greater affinity for CHO-MOR than DAMGO, while PTB had a lower affinity than DAMGO.

## 3.2. *In vivo* studies

### 3.2.1. Hot plate test

In the first *in vivo* experiment, we studied the antinociceptive effect of four i.v. dosages of ITZ (0.0005, 0.001, 0.002, 0.004 mg/kg), fentanyl (0.00125, 0.0025, 0.005, 0.01 mg/kg), morphine (0.5, 1, 2, 4 mg/kg), and the respective vehicle (1 ml/kg). As shown in Figure 4, all the studied MOR

agonists induced dose-dependent analgesia, measured by the latency (s) to hind paw licking or withdrawal response. Two-way ANOVA showed a main effect of treatment ( $F_{(14, 72)}=9.637$ ;  $p<0.0001$ ), time ( $F_{(5.158, 371.4)}= 114.8$ ;  $p<0.0001$ ), and a time  $\times$  treatment interaction ( $F_{(140,720)} = 8.703$ ;  $p<0.0001$ ). Tuckey's *post hoc* tests showed a significant increase in latency: i) after ITZ 0.004 mg/kg treatment with respect to basal value and vehicle (1-30 min), ITZ 0.0005 mg/kg (5-30 min), and ITZ 0.001 mg/kg (15-30 min); ii) after fentanyl 0.01 mg/kg treatment with respect to basal value (1-10 min) and vehicle (1.5 min); iii) after morphine 4.0 mg/kg treatment with respect to basal value (15 min). We also calculated the median effective dose ( $ED_{50}$ ) values with the obtained antinociceptive data. The  $ED_{50}$  of ITZ was about 3.7 times lower than that of fentanyl and about 1500 times lower than that of morphine (Fig. 5).

### 3.2.2. *In vivo* brain microdialysis and behavioral rating score

Rat basal values of NAc shell DA, expressed as fmoles/10 ml sample (mean  $\pm$  SEM), were  $53 \pm 4$  (N =50).

#### 3.2.2.1 Dose-response relationship of intravenous ITZ and MTZ on dialysate NAc shell DA

In the first microdialysis experiment, we studied the effect of three dosages of ITZ (0.001, 0.003, 0.01 mg/kg), and vehicle (1 mL/kg) on dialysate DA in the NAc shell. As shown in Figure 6A, the administration of ITZ 0.01 mg/kg increased dialysate DA with respect to the vehicle and to the lower dosages tested (0.001 and 0.003 mg/kg). Two-way ANOVA showed a main effect of time ( $F_{(3.36, 53.80)} 3.401$ ;  $p<0.05$ ) and dosage ( $F_{(3, 16)} = 9.455$ ;  $p<0.001$ ), and a time  $\times$  dosage interaction ( $F_{(45, 240)} = 2.87$ ;  $p<0.0001$ ). Tuckey's *post hoc* tests showed an increase in dialysate DA after ITZ 0.01 mg/kg with respect to basal value (120 min), to vehicle (20-80, 100-140 min), and to 0.001 mg/kg (20, 80, 120, 160 min), and after ITZ 0.03 mg/kg with respect to vehicle (20-40 min). Moreover, we studied the effect of three i.v. dosages of MTZ (0.001, 0.01, 0.03 mg/kg), and vehicle (1 mL/kg) on dialysate DA in the NAc shell of male SD rats. As shown in Figure 6B, the administration of MTZ 0.03 and 0.01

mg/kg increased DA levels with respect to vehicle and to the lowest dosage tested. Two-way ANOVA showed a main effect of dosage ( $F_{(3, 18)} = 3.77$ ;  $p < 0.05$ ). Tuckey's *post hoc* tests applied to the dosage factor showed a significant increase in dialysate DA after MTZ 0.03 mg/kg with respect to basal value (40 min), to vehicle (40, 80 min), and to 0.001 mg/kg (40, 80 min).

#### 3.2.2.2 Comparison of the effects of intravenous morphine, fentanyl, ITZ, and MTZ on dialysate NAc shell DA

In the second microdialysis experiment, we compared the effect of the higher dosages tested of ITZ (0.01 mg/kg), and MTZ (0.03 mg/kg) with a selected dosage of morphine (1.0 mg/kg) or fentanyl (0.01 mg/kg), and with vehicle (1 ml/kg) on dialysate DA levels in NAc shell. As shown in Figure 7, all the MOR agonists studied increased DA levels with respect to control animals. Two-way ANOVA showed a main effect of treatment ( $F_{(4, 20)} = 4.804$ ;  $p < 0.01$ ), time ( $F_{(4.37, 87.47)} = 8.747$ ;  $p < 0.0001$ ), and a time  $\times$  treatment interaction ( $F_{(60, 300)} = 1.786$ ;  $p < 0.001$ ). Tuckey's *post hoc* tests showed a significant increase in dialysate DA after ITZ treatment with respect to basal value (120 min), to vehicle (20, 40, 80, 100, 120 min), to MTZ (120 min) and to fentanyl (100 min), and after morphine treatment with respect to basal value (40, 60, 120, 140, 180 min) and to vehicle (40, 60, 100, 160, 180 min).

#### 3.2.2.3 Behavioral activity rate after intravenous morphine, ITZ, and MTZ

In order to evaluate behavioral activity 10 min after drug administration, we compared the effects of selected dosages of ITZ (0.01 mg/kg), MTZ (0.03 mg/kg), morphine (1 mg/kg), and vehicle (1 ml/kg). As shown in Figure 8, the administration of all the tested MOR agonists decreased the sedation rating with respect to the vehicle. The Kruskal-Wallis test revealed a significant treatment effect ( $p < 0.001$ ). Dunn's *post hoc* test showed significant differences between ITZ and morphine with respect to the vehicle.

#### 3.2.2.4 Time-course of the behavioral activity after intravenous morphine, ITZ, and MTZ

In order to characterize the time-course of the effect of nitazenes on the sedation rating, three dosages of ITZ (0.001, 0.003, 0.01 mg/kg) and MTZ (0.001, 0.01, 0.03 mg/kg) were administered, and the rate of activity was compared with that observed after administration of the respective vehicle (1 ml/kg), and after morphine (1.0 mg/kg) for 180 min post-drug. As shown in Figure 9, both ITZ and MTZ affected the activity rate in a dose-dependent manner. However, ITZ was more effective than MTZ and displayed a different response pattern when compared to morphine. Two-way ANOVA showed a main effect of treatment ( $F_{(8, 45)} = 35.84$ ;  $p < 0.0001$ ), time ( $F_{(2, 403, 180.1)} = 86.93$ ;  $p < 0.0001$ ), and a treatment  $\times$  time interaction ( $F_{(40, 225)} = 19.25$ ;  $p < 0.0001$ ). Tuckey's *post hoc* tests showed significant differences between ITZ 0.001 mg/kg (30 min), 0.003 mg/kg (30 min), and 0.01 mg/kg (30-90 min), MTZ 0.01 mg/kg (30 min), and 0.03 mg/kg (30, 60 min), when compared with the respective vehicle. Tuckey's *post hoc* tests showed significant differences between morphine and ITZ 0.01 mg/kg (60, 90 min) or MTZ 0.03 mg/kg (30-90 min).

### 3.3. *In silico* studies

#### 3.3.1. *In Silico* Results: IFD, MM-GBSA and MTD experiments

IFD Protocol identified the best binding positions and interactions of the positively charged ITZ, MTZ and PTB along with fentanyl as the reference compound. All compounds showed a key salt bridge interaction with the amino acid Asp 147 (D147) and a  $\pi$ -cation contact with Tyr 148 (Y148). As shown in Figure 10, nitazenes displayed a series of electrostatic  $\pi$ - $\pi\pi$  and  $\pi$ -stacking aromatic interactions with the inner part of the receptor, while PTB showed different aromatic interactions. As regards the large receptor hydrophobic surface, Figure 11 showed that ITZ, MTZ and fentanyl were involved in a larger number of Van der Waals interactions both with the inner and outer part of the receptor pocket and with a hydrophobic sub-pocket. Interestingly, we observed that the presence of the isopropoxy group allowed ITZ to interact more deeply with a larger pocket surface. Also, in view of the MM-GBSA scores, the ITZ-protein complex showed an energy gain greater than the MTZ-protein complex, which, in turn, was better than the PTB-protein complex (Table 3). Moreover, the

MTD experiments reported in Fig. Suppl. 2 and 3, identified ITZ and MTZ as the most stable compounds, whilst PTB, whose degree of motion was twice as high, was the least stable; MTD also revealed that nitazenes were more stable than fentanyl. The electrostatic surface distribution of MOR in the active form showed that ITZ and MTZ interacted more deeply with a larger pocket surface, with ITZ being the most stable inside the pocket (Figures 12A and B). In detail, we observed that the isopropoxy moiety induced a rearrangement of the amino acids, particularly His54, in the extracellular terminal domain (Figure 12C). IFD experiments were also carried out with agonists BU72, MTZ and ITZ on the inactive form of MOR bound to the crystal morphinan antagonist BF0. We observed a structural rearrangement of the TM3 helix (TMH3) D147, M151 and N150 residues, crucial for receptor activation. Interestingly, Figure 13A shows that the agonists BU72, MTZ and ITZ bound to D147 induced an anticlockwise shift of the aminoacidic side chain with a probable consequent growing torsion of TMH3 directly proportional to the agonist activity. As shown in Figure 13B, in IFD experiments carried out on the MOR active form, ITZ and MTZ induced a different M151 flip that might be important in the receptor activation process.

## **Discussion**

The main findings of this study are fourfold: i) ITZ and MTZ are high affinity ligands and potent MOR agonists at both native and recombinant MOR systems; ii) ITZ reduces nociception and behavioral activity in a dose-dependent manner; iii) ITZ and MTZ stimulate *in vivo* DA transmission in the NAc shell within a range of dosages able to reduce behavioral activity, and comparable with the concentration used for *in vitro* studies to determine affinity, potency and efficacy; iv) ITZ and MTZ displayed overall MM-GBSA, IFD and MD ranking scores consistent with *in vitro* MOR binding affinity and potency rank order.

Our *in vitro* findings show that ITZ, MTZ and PTB bind with nano/picomolar affinity to MOR in rat cerebral cortex homogenates and in CHO-MOR membranes. Moreover, they show high potency



and efficacy in stimulating the [<sup>35</sup>S]GTPγS binding induced by MOR activation in native and recombinant systems.

To our knowledge, this is the first study that compares the binding affinity and functional activity of nitazenes at the MOR in recombinant (MOR transfected CHO cells) and native systems (brain tissue membranes). The ability to express cloned cDNAs **receptor** in various cell types has provided a powerful tool for studying the binding interaction between ligands and receptors and their function at G protein coupled receptors (GPCRs), e.g., opioid receptors. More specifically, since most of the **opioid agonists** bind and activate all known opioid receptors (δ-, κ- or μ), the use of transfected MOR-CHO makes it possible to selectively characterize the affinity, the potency, and the efficacy of these compounds at the MOR. The receptors expressed in heterologous cell systems frequently have functional properties remarkably similar to those in their native tissue of origin: however, this is not always the case. **For example, in recombinant receptor systems, changes in receptor expression levels (i.e., over/under-expression) can reveal differential potency in displacing agonist and antagonist radioligands thus affecting affinity binding sites due to the limited availability of G proteins, and directly change the cellular mechanisms controlled by agonists, thereby precluding classifications of receptor types with cytosolic processes (see Kenakin 1997 for a review).**

Therefore, to allow the broad characterization of our compounds, the comparison of results obtained from studies of cloned receptors in heterologous systems with the properties of receptors in native tissues was considered of utmost importance. Here, as expected, our reference compound DAMGO acts as a full agonist with nanomolar affinity, potency and high efficacy in both systems (Selley et al. 1998; Zador et al., 2017). However, DAMGO, probably due to its intrinsic properties that might determine the level of receptor activation and the balance between **G protein** activation and inactivation (e.g., phosphorylation, β-arrestin binding and internalization of receptor), shows a lower potency compared to its affinity in both systems. On the other hand, our study has demonstrated that the EC<sub>50</sub> of DAMGO is consistent with that reported by other authors in both rat thalamus and whole brain membranes (Selley et al., 1997), where it displays less potency than affinity (Zador et

al., 2017). Moreover, we reported that  $K_i$  values for DAMGO, but not for nitazenes, are higher in native than in recombinant systems. Conversely, the MOR expression is higher in CHO-MOR than in brain tissue. To the best of our knowledge no other studies has ever reported the comparison between  $K_i$  value of DAMGO and nitazenes in native and CHO-MOR, further investigations are needed to clarify the matter.

In our hands, fentanyl is a MOR full agonist in rat cortex membranes where it displays a higher potency, but lower affinity than DAMGO. The G protein recruitment induced by all compounds is completely suppressed by the MOR antagonist NAL. Taken together, these data indicate that ITZ, MTZ and PTB activate a G protein coupled MOR.

Our radioligand binding results represent the first investigation of these nitazenes in native membranes and in CHO-MOR. In these systems, the use of [ $^3\text{H}$ ]DAMGO allowed us to demonstrate that ITZ and MTZ respectively display a higher or similar binding affinity at MOR as compared to DAMGO. In rat cortical membranes we found that the most potent ITZ and MTZ compounds possess greater agonist potency (about 300- and 16-fold, respectively) compared to DAMGO. Additionally, considering the  $EC_{50}$ s of ITZ and MTZ versus that of fentanyl in rat cortical membranes, our data reveal that the potency of these compounds exceeds that of fentanyl (about 125- and 6-fold higher, respectively). Our results confirm and extend recent *in vitro* reports that used two *in vitro* cell-based recruitment assays, MOR- $\beta$ arr2 and MOR-mini-Gi and showed that ITZ, MTZ and PTB activate MOR with nanomolar potency (Blanckaert et al., 2020; Vandeputte et al., 2020; Vandeputte et al., 2021a). In addition, previous reports show that ITZ and MTZ are less potent than the prototypical drug in this series, etonitazene (for a review see Ujváry et al., 2021). Moreover, while potency data are available for ITZ (Vandeputte et al., 2021a) and N-piperidinyl etonitazene (Vandeputte et al., 2022) in separate publications, a direct comparison between both has not been performed to date. Moreover, despite different systems used among different laboratories, the ranking of binding affinity of nitazenes can be summarized as follows: etonitazene (0.00042-0.11 nM, see Ujváry et al. for more details) > ITZ ( $K_i$ : 0.06 nM and 0.05 in rat brain and CHO-MOR, respectively; present data) > MTZ

( $K_i$ : 0.22 nM and 0.23 in rat brain and CHO-MOR, respectively, present data) > *N*-Pyrrolidino etonitazene ( $k_i$ : 4.09 nM, rat brain tissue, Vanderputte et al., 2022b) > *N*-Piperidinyl etonitazene ( $K_i$ : 14.3 nM, rat brain tissue, Vanderputte et al., 2022a).

Although it has been reported that  $K_i$  values are not always correlated with *in vitro* measurements of potency (Baumann, Kopajtic and Madras 2018; Vanderputte et al. 2022a), we showed that, except for DAMGO, there is a good correspondence between the  $K_i$  and  $EC_{50}$  values of these compounds obtained in CHO-MOR and rat cortical membranes. This finding is in accordance with Lalovic et al. (2006) who found that oxycodone and its metabolites exhibit the same rank order of potency for the activation of [ $^{35}$ S]GTP $\gamma$ S binding to CHO-MOR ( $EC_{50}$ ) as the receptor binding affinity ( $K_i$ ). Similarly, other authors reported that the binding affinity of endogenous and exogenous MOR agonists (alfentanil, fentanyl, loperamide, methadone, meperidine, morphine, and sufentanil) closely matches the potency ( $EC_{50}$  value) (Alt et al., 1998; Kalvass et al., 2007).

Among the NSOs tested *in vitro*, ITZ and MTZ were selected for *in vivo* studies and their effects were compared with those of fentanyl or morphine. Here we showed that ITZ has long lasting dose-dependent analgesic properties at dosages lower than both fentanyl and morphine. In this respect, the antinociceptive  $ED_{50}$  values obtained suggest that ITZ is about three- and a thousand-times more potent than fentanyl and morphine, respectively. Our results are in agreement with previous studies that showed that ITZ has more potent (>500 times) morphine-like centrally mediated analgesic effects in an animal model of experimentally induced pain (Hunger et al., 1957, 1960a, 1960b). Likewise, Lee and colleagues (2022) showed that ITZ exhibited a prolonged half-life in mice compared to fentanyl (about 1.64 vs 0.8 h) and its  $ED_{50}$  was 20  $\mu$ g/kg i.p. for both hot-plate and tail-flick tests. More recently, Baumann and colleagues (2022) also showed that ITZ produced dose-dependent increases in hot plate latency ( $ED_{50}$ =4.2  $\mu$ g/kg) and catalepsy ( $ED_{50}$ =8.7  $\mu$ g/kg), while 30  $\mu$ g/kg produced marked hypothermia.

It has been established that all drugs of abuse exert their rewarding properties by increasing DA transmission specifically in the NAc shell (Di Chiara et al., 2004), ITZ and MTZ were therefore

also evaluated for their *in vivo* DA releasing properties, as estimated by DA microdialysis. Our findings demonstrate that ITZ stimulates DA transmission in the NAc shell in a dose-dependent manner with a maximal effect after 0.01 mg/kg i.v. Notably, this effect was higher than that observed after the same dosage of fentanyl and after 1 mg/kg i.v. of morphine. While previous studies have already examined the effect of morphine (Pontieri et al., 1995; Cadoni and Di Chiara, 1999) and fentanyl (Yoshida et al. 1999) on NAc shell DA by means of microdialysis, this is, to our knowledge, the first preclinical study on the effect of ITZ and MTZ on mesolimbic DA transmission.

In parallel with the measurement of NAc shell DA, we utilized an observational rating scale in order to evaluate behavioral activity from 10 to 180 min post-drug. We utilized this method to avoid any interference with the microdialysis experimental setup, where rats are placed in a plastic bowl and connected to a line of tubing that limited their locomotion. We observed that ITZ decreased behavioral activity dose-dependently, with the highest effect observed after the administration of 0.01 mg/kg i.v., whilst a milder reduction was observed after MTZ 0.03 mg/kg. Notably, the effects observed 10 min after the highest dosages of ITZ and MTZ are significantly different, while the effects of ITZ are comparable with those observed after 1 mg/kg i.v. of morphine. Interestingly, behavioral observation for 3 consecutive hours disclosed a different profile of the highest dosage of ITZ tested (0.01 mg/kg i.v.) as compared to morphine (1 mg/kg i.v.). Thus, while the initial reduction of activity induced by morphine progressively fades away by 30 min post-drug, the sedative effect of ITZ lasts up to 120 min, with a score of 1.2-2.1. The doses of ITZ and morphine that increase extracellular DA produce robust sedation. Nevertheless, this fact does not impact on the interpretation of the findings since reward signaling and sedation are not encoded by the same neural pathways. In particular, opioids stimulate DA release in the nucleus accumbens (NAc) shell by blocking the inhibition exerted by GABA neurons onto DA neurons in the Ventral Tegmental Area (VTA); this effect is regulated by MOR receptors expressed in the GABA neurons and was also demonstrated in anesthetized animals (Bonci and Williams, 1996; Jalabert et al, 2011; Lecca et al, 2012; Meye et al, 2012).

*In silico* IFD studies carried out on the MOR active form showed that most energetically favored fentanyl-MOR complex pose occurred with the amide group oriented toward TMH 6 and the N-phenyl ethyl chain directed to TMH3, in agreement with previous findings (Ricarte et al., 2021; Xie et al., 2022). As far as the compounds under investigation are concerned, IFD experiments revealed that PTB, the smallest molecule under study, interacted both with the hydrophobic sub-pocket and the inner part of the receptor but very poorly with the outer part of the pocket, also showing a less stable pose and, perhaps, a shorter permanence in the receptor. Moreover, the ITZ isopropoxy moiety induced an amino acid rearrangement in the extracellular terminal domain that stabilized the receptor site in a closed form, thereby preventing the entrance of other ligands (i.e., DAMGO). This fact might also be related to the higher potency of ITZ towards MTZ. To deeply investigate the receptor conformational features involved in the activation mechanism, IFD experiments were also carried out with agonists BU72, MTZ and ITZ on the inactive form of MOR bound to the crystal morphinan antagonist BF0. Results coherently match with the MD simulations performed on MOR crystal during receptor activation (Huang et al., 2015). Notably, with respect to PTB, ITZ, MTZ and fentanyl displayed more energetically favorable poses related to a higher number of both electrostatic and hydrophobic interactions.

In conclusion, we have shown that ITZ and MTZ are highly potent and effective agonists of MOR receptors and, consistent with the properties of fentanyl and morphine, they activate DA transmission in the rat NAc shell. These *in vitro* and *in vivo* observations may be supported by *in silico* data which suggests that since ITZ gains contact with a wider part of the pocket hydrophobic surface, it may stabilize the receptor in a more closed form that allows a longer permanence of the ligand and, consequently, a greater agonistic activity.

## ACKNOWLEDGEMENT

The authors gratefully thank Dr. Gessica Piras for the technical support during in vivo experiments.

### CRedit authorship contribution statement

**Maria Antonietta De Luca:** In vivo investigation, Formal Analysis, Conceptualization, Writing – original draft- review & editing. **Graziella Tocco:** Validation, In silico Investigation, formal analysis. **Rafaela Mostallino:** In vitro Investigation, Formal Analysis; **Antonio Laus:** In silico Investigation, Formal Analysis. **Francesca Caria:** In vivo Investigation. **Aurora Musa:** In vivo Investigation. **Nicholas Pintori:** Statistical analysis and graphical revision. **Marcos Ucha:** Behavioral evaluation. **Celia Poza:** Behavioral evaluation. **Emilio Ambrosio:** Validation, Behavioral evaluation, Formal Analysis. **Gaetano Di Chiara:** Conceptualization, Supervision, Writing – review & editing. **M Paola Castelli:** Conceptualization, In vitro Investigation, Writing – review & editing.

### Conflicts of interest

The authors declare that they have no known competing financial interests or personal relationships that might have appeared to influence the work reported in this paper.

## References

Adamson, D.W., Green, A.F., 1950. A new series of analgesics. *Nature* 165(4186):122–122. doi: 10.1038/165122a0

Adamson, D., Duffin, W., Green, A., 1951. Dithienylbutylamines as Analgesics. *Nature* 167, 153–154. <https://doi.org/10.1038/167153b0>

Alt, A., Mansour, A., Akil, H., Medzihradsky, F., Traynor, J.R., Woods, J.H., 1998. Stimulation of guanosine-5'-O-(3-[35S]thio)triphosphate binding by endogenous opioids acting at a cloned mu receptor. *J. Pharmacol. Exp. Ther.* 286, 282-288. PMID: 9655870.

Arillotta, D., Schifano, F., Napoletano, F., Zangani, C., Gilgar, L., Guirguis, A., Corkery, J.M., Aguglia, E., Vento, A., 2020. Novel Opioids: Systematic Web Crawling Within the e-Psychnonauts' Scenario. *Front. Neurosci.* 18, 14:149. doi: 10.3389/fnins.2020.00149.

Baumann, M.H., Kopajtic, T.A., Madras, B.K., 2018. Pharmacological Research as a Key Component in Mitigating the Opioid Overdose Crisis. *Trends Pharmacol. Sci.* <https://doi.org/10.1016/j.tips.2018.09.006>

Baumann, M.H., Pasternak, G.W., 2018. Novel Synthetic Opioids and Overdose Deaths: Tip of the Iceberg? *Neuropsychopharmacology.* <https://doi.org/10.1038/npp.2017.211>

Baumann, M.H., Glatfelter G.C., Walther D., Walton S.E., Logan, B.K., Krotulski A.J., 2022. Pharmacodynamics and Pharmacokinetics of the Non-Fentanyl Synthetic Opioid, Isotonitazene, in Male Rats. *FASEB J.* <https://doi.org/10.1096/fasebj.2022.36.S1.R3857>. Abstract presented at the Experimental Biology meeting.

Blanckaert, P., Cannaert, A., Van Uytvanghe, K., Hulpia, F., Deconinck, E., Van Calenbergh, S., Stove, C., 2020. Report on a novel emerging class of highly potent benzimidazole NPS

- opioids: Chemical and in vitro functional characterization of isotonitazene. *Drug Test. Anal.* 12, 422–430. <https://doi.org/10.1002/dta.2738>
- Bolan, E.A., Pan, Y.X., Pasternak, G.W., 2004. Functional Analysis of MOR-1 Splice Variants of the Mouse  $\mu$  Opioid Receptor Gene. *Opn. Synapse* 51, 11–18. <https://doi.org/10.1002/syn.10277>
- Bonci, A., Williams, J.T., 1996. A common mechanism mediates long-term changes in synaptic transmission after chronic cocaine and morphine. *Neuron* 16, 631–639.
- Bradford, M.M., 1976. A rapid and sensitive method for the quantitation of microgram quantities of protein utilizing the principle of protein-dye binding. *Anal. Biochem.* 72, 248–254. [https://doi.org/10.1016/0003-2697\(76\)90527-3](https://doi.org/10.1016/0003-2697(76)90527-3)
- Bromig, G., 1958. Über neue starkwirkende Analgetika und ihre klinische Erprobung. *Klin. Wochenschr.* 36, 960–963. <https://doi.org/10.1007/BF01486702>
- Cadoni, C., Di Chiara, G., 1999. Reciprocal changes in dopamine responsiveness in the nucleus accumbens shell and core and in the dorsal caudate-putamen in rats sensitized to morphine. *Neuroscience* 90, 447–455. doi: 10.1016/s0306-4522(98)00466-7. PMID: 10215150.
- Cheng Y., Prusoff W.H., 1973. Relationship between the inhibition constant (K<sub>1</sub>) and the concentration of inhibitor which causes 50 per cent inhibition (I<sub>50</sub>) of an enzymatic reaction. *Biochem. Pharmacol.* 22(23):3099-108. doi: 10.1016/0006-2952(73)90196-2
- De Luca, M.A, Valentini, V., Bimpisidis, Z., Cacciapaglia, F., Caboni, P., Di Chiara, G., 2014. Endocannabinoid 2-Arachidonoylglycerol Self-Administration by Sprague-Dawley Rats and



- Stimulation of in vivo Dopamine Transmission in the Nucleus Accumbens Shell. *Front. Psychiatry* 17; 5:140. doi: 10.3389/fpsyt.2014.00140.
- De Luca, M.A., Castelli, M.P., Loi, B., Porcu, A., Martorelli, M., Miliano, C., Kellett, K., Davidson, C., Stair, J.L., Schifano, F., Di Chiara, G., 2016. Native CB1 receptor affinity, intrinsic activity and accumbens shell dopamine stimulant properties of third generation SPICE/K2 cannabinoids: BB-22, 5F-PB-22, 5F-AKB-48 and STS-135. *Neuropharmacology* Jun;105:630-638. doi: 10.1016/j.neuropharm.2015.11.017. Epub 2015 Dec 11. PMID: 26686391. 20162016
- De Luca, M.A., Di Chiara G., 2019. Strategies of intervention to limit the novel synthetic opioids (NSO) escalation in Europe. *Research and Advances in Psychiatry* 6(2):40-42
- Deneau, G. A., McCarthy, D. A., Seevers, M. H., 1959. Addendum 1. Physical dependence liability studies in the monkey. 20th Meeting Committee on Drug Addiction and Narcotics, National Academy of Sciences - National Research Council, Washington D.C., 1–13.
- Deuis, J.R., Dvorakova, L.C., Vetter, I., 2017. Methods Used to Evaluate Pain Behaviors in Rodents. *Front. Mol. Neurosci.*, Vol. 10; 06 September 2017. <https://doi.org/10.3389/fnmol.2017.00284>.
- Di Chiara, G., Bassareo, V., Fenu, S., De Luca, M.A., Spina, L., Cadoni, C., et al., 2004. Dopamine and drug addiction: the nucleus accumbens shell connection. *Neuropharmacology* 47 (Suppl. 1), 227e241. Review.
- European Monitoring Centre for Drugs and Drug Addiction, 2020. Risk assessment report on the new psychoactive substance N,N-diethyl-2-[[4-(1-methylethoxy)phenyl]methyl]-5-nitro-1H-benzimidazole-1-ethanamine (isotonitazene) in accordance with Article 5c of Regulation

(EC) No 1920/2006 (as amended), Risk Assessments, Publications Office of the European Union, Luxembourg. <https://www.emcdda.europa.eu/publications/risk-assessments/>

European Monitoring Centre for Drugs and Drug Addiction, 2020. European Drug Report 2020: Trends and Developments, Publications Office of the European Union, Luxembourg Available online: [https://www.emcdda.europa.eu/system/files/publications/13236/TDAT20001ENN\\_web.pdf](https://www.emcdda.europa.eu/system/files/publications/13236/TDAT20001ENN_web.pdf) (accessed on 06 March 2022)

European Monitoring Centre for Drugs and Drug Addiction. *European Drug Report 2021*. European Union Publications Office: Lisbon, 2021. Available online: [http://www.emcdda.europa.eu/system/files/publications/4541/TDAT17001ENN.pdf\\_en](http://www.emcdda.europa.eu/system/files/publications/4541/TDAT17001ENN.pdf_en) (accessed on 06 March 2022)

European Monitoring Centre for Drugs and Drug Addiction. *New psychoactive substances: global markets, global threats and the COVID-19 pandemic*. An update from the EU Early Warning System, 2020. Available online: [https://www.emcdda.europa.eu/system/files/publications/13464/20205648\\_TD0320796ENN\\_PDF\\_rev.pdf](https://www.emcdda.europa.eu/system/files/publications/13464/20205648_TD0320796ENN_PDF_rev.pdf) (accessed on 06 March 2022).

European Monitoring Centre for Drugs and Drug Addiction. *Spotlight on... Fentanils and other new opioids*, 2021. Available online: [https://www.emcdda.europa.eu/spotlights/fentanils-and-other-new-opioids\\_en](https://www.emcdda.europa.eu/spotlights/fentanils-and-other-new-opioids_en) (accessed on 06 March 2022)

Fusani, L., Palmer, D.S., Somers, D.O., Wall, I.D., 2020. Exploring Ligand Stability in Protein Crystal Structures Using Binding Pose Metadynamics. *J. Chem. Inf. Model.* 60(3):1528-1539. doi: 10.1021/acs.jcim.9b00843

Gillan, M.G.C., Kosterlitz, H.W., 1982. Spectrum of the M-,  $\Delta$ - and K- Binding Sites in Homogenates of Rat Brain. *Br. J. Pharmacol.* 77, 461–469. <https://doi.org/10.1111/j.1476-5381.1982.tb09319.x>

Green, A.F., 1953. Analgesic and other properties of 3: 3-dithienylalkenylamines. *Br. J. Pharmacol. Chemother.* 8(1):2-9. doi: 10.1111/j.1476-5381.1953.tb00739.x.

Greenwood, J.R., Calkins, D., Sullivan, A.P., Shelley, J.C., 2010. Towards the comprehensive, rapid, and accurate prediction of the favorable tautomeric states of drug-like molecules in aqueous solution. *J. Comput. Aided. Mol. Des.* 24(6-7):591-604. doi: 10.1007/s10822-010-9349-1

Gross, F., and Turrian, H., 1957. Über Benzimidazolderivate mit starker analgetischer Wirkung. *Experientia* 13 (10), 401–403.

Harder, E., Damm, W., Maple, J., Wu, C., Reboul, M., Xiang, J.Y., Wang, L., Lupyan, D., Dahlgren, M.K., Knight, J.L., Kaus, J.W., Cerutti, D.S., Krilov, G., Jorgensen, W.L., Abel, R., Friesner, R.A., 2016. OPLS3: A Force Field Providing Broad Coverage of Drug-like Small Molecules and Proteins. *J. Chem. Theory Comput.* 12(1):281-96. doi: 10.1021/acs.jctc.5b00864

Hoffmann, K., Hunger, A., and Rossi, A., 1960. Benzimidazoles. U.S. Patent 2935514A.

<https://bluelight.org/xf/search/1916937/?q=isotonitazenes&o=relevance>

[https://drugsforum.com/search/2828360/?q=isotonitazene&o=relevance&c\[p\]\[vwcomment\]\[display\\_order\]=0](https://drugsforum.com/search/2828360/?q=isotonitazene&o=relevance&c[p][vwcomment][display_order]=0)

<https://www.cdc.gov/nchs/nvss/vsrr/drug-overdosedata.htm>

<https://www.federalregister.gov/documents/2022/04/12/2022-07640/schedules-of-controlled-substances-temporary-placement-of-butonitazene-etodesnitazene-flunitazene>

- Huang, W., Manglik, A., Venkatakrisnan, A.J., Laeremans, T., Feinberg, E.N., Sanborn, A.L., Kato, H.E., Livingston, K.E., Thorsen, T.S., Kling, R.C., Granier, S., Gmeiner, P., Husbands, S.M., Traynor, J.R., Weis, W.I., Steyaert, J., Dror, R.O., Kobilka, B.K., 2015. Structural insights into  $\mu$ -opioid receptor activation. *Nature* 524:315-21. doi: 10.1038/nature14886.
- Hunger, A., Kebrle, J., Rossi, A., Hoffmann, K., 1957. Synthese basisch substituierter, analgetisch wirksamer Benzimidazol-derivate. *Experientia* 13 (10) 400-401.
- Hunger, A., Kebrle, J., Rossi, A., Hoffmann, K., 1960a. Benzimidazol- Derivate und verwandte Heterocyclen III. Synthese von 1- Aminoalkyl- 2- nenzyl- nitro- benzimidazolen. *Helv. Chim. Acta* 43, 1032–1046. <https://doi.org/10.1002/hlca.19600430412>.
- Hunger, A., Kebrle, J., Rossi, A., Hoffmann, K., 1960b. ‘Benzimidazol-Derivate und verwandte Heterocyclen. II. Synthese von 1-Aminoalkyl-2-benzyl-benzimidazolen’, *Helv. Chim. Acta* 43, 800–809.
- Jalabert, M., Bourdy, R., Courtin, J., Veinante, P., Manzoni, O.J., Barrot, M., Georges, F., 2011. Neuronal circuits underlying acute morphine action on dopamine neurons. *Proc. Natl. Acad. Sci. USA* 108,16446–16450.
- Kase, Y., Kaku, T., Yamamoto, Y., Tanaka, M., Takasaki, Y., Nagao, K., 1955. 3-Piperidyl-1, 1-di(2'-thienyl)-but-1-ene as a potent antitussive. *Pharm. Bull.* 3(5):395-6.
- Kimura, R., Yabuuchi, T., Tamura, Y., 1958. Studies on thiophene derivatives. I. Syntheses of 2-amino-1,1-di(2-thienyl)alkanols. *Chem. Pharm. Bull. (Tokyo)*. 6, 159-163. doi: 10.1248/cpb.6.159. PMID: 13537176.

- Kalvass, J.C., Olson, E.R., Cassidy, M.P., Selley, D.E., Pollack, G.M., 2007. Pharmacokinetics and pharmacodynamics of seven opioids in P-glycoprotein-competent mice: assessment of unbound brain EC<sub>50</sub>,u and correlation of in vitro, preclinical, and clinical data. *J. Pharmacol. Exp. Ther.* 323, 346-55. doi: 10.1124/jpet.107.119560. Epub 2007 Jul 23. PMID: 17646430.
- Kenakin, T., 1997. Differences between natural and recombinant G protein-coupled receptor systems with varying receptor/G protein stoichiometry. *Trends Pharmacol. Sci.*18:456-464. doi: 10.1016/s0165-6147(97)01136-x. PMID: 9458693.
- Krotulski, A.J., Papsun, D.M., Kacinko, S.L., Logan, B.K., 2020. Isotonitazene Quantitation and Metabolite Discovery in Authentic Forensic Casework. *J. Anal. Toxicol.* 44, 521–530. <https://doi.org/10.1093/JAT/BKAA016>
- Krotulski, A.J., Papsun, D.M., Walton, S.E., Logan, B.K., 2021. Metonitazene in the United States Forensic toxicology assessment of a potent new synthetic opioid using liquid chromatography mass spectrometry. *Drug Test. Anal.* 13, 1697–1711. <https://doi.org/10.1002/dta.3115>
- Lalovic, B., Kharasch, E., Hoffer, C., Risler, L., Liu-Chen, L.Y., Shen, D.D. 2006. Pharmacokinetics and pharmacodynamics of oral oxycodone in healthy human subjects: role of circulating active metabolites. *Clin Pharmacol Ther.* 461-479. doi: 10.1016/j.clpt.2006.01.009. PMID: 16678548.
- Lecca, S., Melis, M., Luchicchi, A., Ennas, M.G., Castelli, M.P., Muntoni, A.L., Pistis, M. 2011. Effects of drugs of abuse on putative rostromedial tegmental neurons, inhibitory afferents to midbrain dopamine cells. *Neuropsychopharmacology*, 36:589-602. doi: 10.1038/npp.2010.190. Epub 2010 Nov 3. PMID: 21048703; PMCID: PMC3055682. 2011

- Lee, J. C., Park, H., Eubanks, L. M., Ellis, B., Zhou, B., Janda, K.D., 2022. A Vaccine against Benzimidazole-Derived New Psychoactive Substances That Are More Potent Than Fentanyl-*Journal of Medicinal Chemistry*65 (3), 2522-2531 DOI: 10.1021/acs.jmedchem.1c01967
- Logan, B. K., Krotulski, A. J., Papsun, D. M., and Kacinko, S. L., 2020. Isotonitazene: a novel benzimidazole  $\mu$ -opioid agonist as the latest novel opioid. [https://www.npsdiscovery.org/wp-content/uploads/2020/10/Logan\\_Isotonitazene-Presentation\\_SOFT-2020.pdf](https://www.npsdiscovery.org/wp-content/uploads/2020/10/Logan_Isotonitazene-Presentation_SOFT-2020.pdf) (accessed on 24 February 2021).
- Manglik, A., Kruse, A.C., Kobilka, T.S., Thian, F.S., Mathiesen, J.M., Sunahara, R.K., Pardo, L., Weis, W.I., Kobilka, B.K., Granier, S., 2012. Crystal structure of the  $\mu$ -opioid receptor bound to a morphinan antagonist. *Nature* 485, 321-326. doi: 10.1038/nature10954.
- Meye, F.J., van Zessen, R., Smidt, M.P., Adan, R.A., Ramakers, G.M. 2012. Morphine withdrawal enhances constitutive mu-opioid receptor activity in the ventral tegmental area. *J Neurosci* 32, 16120–16128.
- Mueller, F., Bogdal, C., Pfeiffer, B., Andrello, L., Ceschi, A., Thomas, A., Grata, E., 2021. Isotonitazene: Fatal intoxication in three cases involving this unreported novel psychoactive substance in Switzerland. *Forensic. Sci. Int.* 320:110686. doi: 10.1016/j.forsciint.2021.110686
- Paxinos, G., Watson, C., 2007. *The rat brain in stereotaxic coordinates*. Academic Press/Elsevier.
- Pontieri, F.E., Tanda, G., Di Chiara, G., 1995. Intravenous cocaine, morphine, and amphetamine preferentially increase extracellular dopamine in the "shell" as compared with the "core" of the rat nucleus accumbens. *Proc. Natl. Acad. Sci. USA* 92, 12304-12308. doi: 10.1073/pnas.92.26.12304. PMID: 8618890; PMCID: PMC40345.

Porcu, A., Melis, M., Turecek, R., Ullrich, C., Mocci, I., Bettler, B., Gessa, G.L., Castelli, M.P., 2018.

Rimonabant, a potent CB1 cannabinoid receptor antagonist, is a G<sub>ai/o</sub> protein inhibitor. *Neuropharmacology* 133,107-120. doi: 10.1016/j.neuropharm.2018.01.024. PMID: 29407764.

Prekupec, M.P., Mansky, P.A., Baumann, M.H., 2017. Misuse of Novel Synthetic Opioids: A Deadly New Trend. *J. Addict. Med.* 11, 256-265. doi: 10.1097/ADM.0000000000000324. PMID: 28590391; PMCID: PMC5537029.

Ricarte, A., Dalton, J.A.R., Giraldo, J., 2021 Structural Assessment of Agonist Efficacy in the  $\mu$ -Opioid Receptor: Morphine and Fentanyl Elicit Different Activation Patterns. *J Chem Inf Model.* 2021 Mar 22;61(3):1251-1274. doi: 10.1021/acs.jcim.0c00890. Epub 2021 Jan 15. PMID: 33448226.

Rossi, A., Hunger, A., Kebrle, J., Hoffmann, K., 1960. Benzimidazol- Derivate und verwandte Heterocyclen. IV. Die Kondensation von o- Phenylendiamin mit  $\alpha$ - Aryl- und  $\gamma$ - Aryl-acetessigester. *Helv. Chim. Acta* 43, 1046–1056. <https://doi.org/10.1002/hlca.19600430413>

Salamone, J.D., Cousins, M.S., Maio, C., Champion, M., Turski, T., Kovach, J., 1996. Different behavioral effects of haloperidol, clozapine and thioridazine in a concurrent lever pressing and feeding procedure. *Psychopharmacology (Berl.)* 125, 105–112. <https://doi.org/10.1007/BF02249408>

Sastry, G.M., Adzhigirey, M., Day, T., Annabhimoju, R., Sherman, W., 2013. Protein and ligand preparation: parameters, protocols, and influence on virtual screening enrichments. *J. Comput. Aided. Mol. Des.* 27(3):221-34. doi: 10.1007/s10822-013-9644-8

Schrödinger Release 2021-1: Maestro, Schrödinger, LLC, New York, NY, 2021.

Schrödinger Release 2021-1: Protein Preparation Wizard; Epik, Schrödinger, LLC, New York, NY, 2021; Impact, Schrödinger, LLC, New York, NY; Prime, Schrödinger, LLC, New York, NY, 2021.

Schrödinger Release 2021-1: LigPrep, Schrödinger, LLC, New York, NY, 2021.

Schrödinger Release 2021-1: Epik, Schrödinger, LLC, New York, NY, 2021.

Schrödinger Release 2021-1: Induced Fit Docking protocol; Glide, Schrödinger, LLC, New York, NY, 2021; Prime, Schrödinger, LLC, New York, NY, 2021.

Schrödinger Release 2021-1: Prime, Schrödinger, LLC, New York, NY, 2021.

Schrödinger Release 2021-1: Desmond Molecular Dynamics System, D. E. Shaw Research, New York, NY, 2021. Maestro-Desmond Interoperability Tools, Schrödinger, New York, NY, 2021.

Selley, D.E., Sim, L.J., Xiao, R., Liu, Q., Childers, S.R., 1997.  $\mu$ -Opioid receptor-stimulated guanosine-5'-O-( $\gamma$ -thio)-triphosphate binding in rat thalamus and cultured cell lines: signal transduction mechanisms underlying agonist efficacy. *Mol. Pharmacol.* 51, 87-96. doi: 10.1124/mol.51.1.87. PMID: 9016350.

Selley, D.E., Liu, Q., Childers, S.R., 1998. Signal transduction correlates of  $\mu$  opioid agonist intrinsic efficacy: Receptor-stimulated [ $^{35}$ S]GTP $\gamma$ S binding in mMOR-CHO cells and rat thalamus. *J. Pharmacol. Exp. Ther.* 285, 496–505.

Seyler, T., Giraudon, I., Noor, A., Mounteney, J., Griffiths, P., 2021. Is Europe facing an opioid epidemic: What does European monitoring data tell us? *Eur. J. Pain (United Kingdom)* 25, 1072–1080. <https://doi.org/10.1002/ejp.1728>



Sherman, W., Day, T., Jacobson, M.P., Friesner, R.A., Farid, R., 2006. Novel procedure for modeling ligand/receptor induced fit effects. *J. Med. Chem.* 49(2):534-53 doi: 10.1021/jm050540c

Shover, C.L., Falasinnu, T.O., Freedman, R.B., Humphreys, K., 2021. Emerging Characteristics of Isotonitazene-Involved Overdose Deaths: A Case-Control Study. *J. Addict. Med.* 15(5):429-431. doi: 10.1097/ADM.0000000000000775

Ujváry, I., 2020. 'Technical review of new synthetic opioids identified on the European drug market. Part 1. Benzimidazole opioids', EMCDDA Contract Code CT.20.SAS.00017.1.0

Ujváry, I., Christie, R., Evans-Brown, M., Gallegos, A., Jorge, R., de Morais, Sedefov, R., 2021. DARK Classics in Chemical Neuroscience: Etonitazene and Related Benzimidazoles. *ACS Chemical Neuroscience* 12 (7), 1072-1092. DOI: 10.1021/acchemneuro.1c00037

UNODC (2021) CND Decision on international control of isotonitazene enters into force. In: <https://www.unodc.org/LSS/announcement/Details/65247392-26c7-4446-a2b6-270226103036>. (Accessed on 10 June 2021)

United States Drug Enforcement Administration–Veterans Affairs Interagency Agreement. Isotonitazene.N,N-diethyl-2-[[4-(1-methylethoxy)phenyl]methyl]-5-nitro-1H-benzimidazole-1-ethanamine. Binding and functional activity at delta, kappa and mu opioid receptors. In vitro receptor and transporter assays for abuse liability testing for the Drug Enforcement Administration by the Veterans Affairs. Springfield, 2019.

Vandeputte, M.M., Cannart, A., Stove, C.P., 2020. In vitro functional characterization of a panel of non-fentanyl opioid new psychoactive substances. *Arch. Toxicol.* 94, 3819–3830. <https://doi.org/10.1007/s00204-020-02855-7>

Vandeputte, M.M., Van Uytfanghe, K., Layle, N.K., St. Germaine, D.M., Iula, D.M., Stove, C.P., 2021a. Synthesis, Chemical Characterization, and  $\mu$ -Opioid Receptor Activity Assessment of the Emerging Group of “nitazene” 2-Benzylbenzimidazole Synthetic Opioids. ACS Chem. Neurosci. 12, 1241–1251. <https://doi.org/10.1021/acchemneuro.1c00064>

Vandeputte, M.M., Krotulski, A.J., Papsun, D.M., Logan, B.K., Stove, C.P., 2021b. The Rise and Fall of Isotonitazene and Brorphine: Two Recent Stars in the Synthetic Opioid Firmament. J. Anal. Toxicol. Jul 8:bkab082. doi: 10.1093/jat/bkab082. Epub ahead of print. PMID: 34233349.

Vandeputte, M.M., Verougstraete, N., Walther, D., Glatfelter, G.C., Malfliet, J., Baumann, M.H., Verstraete, A.G., Stove, C.P., 2022a. First identification, chemical analysis and pharmacological characterization of N-piperidinyl etonitazene (etonitazepipne), a recent addition to the 2-benzylbenzimidazole opioid subclass. Arch. Toxicol. 96, 1865-1880. doi: 10.1007/s00204-022-03294-2. Epub 2022 Apr 21. PMID: 35449307.

Vandeputte, M.M., Krotulski, A.J., Walther, D., Glatfelter, G.C., Papsun, D., Walton, S.E., Logan, B.K., Baumann, M.H., Stove C,P. 2022b Pharmacological evaluation and forensic case series of N-pyrrolidino etonitazene (etonitazepyne), a newly emerging 2-benzylbenzimidazole 'nitazene' synthetic opioid. Arch Toxicol. 96, 1845-1863. doi: 10.1007/s00204-022-03276-4. Epub 2022 Apr 28. PMID: 35477798.

Volkow, N.D., Wang, G.J., Fowler, J.S., Tomasi, D., 2012. Addiction circuitry in the human brain. Annu. Rev. Pharmacol. Toxicol. 52, 321-336. <http://dx.doi.org/10.1146/annurev-pharmtox-010611-134625>. Review. Epub 2011 Sep 27.

World Health Organization. Critical Review Report: ISOTONITAZENE, 2020.

<https://www.who.int/docs/default-source/controlled-substances/43rd-ecdd/isonitazene-43rd-final-complete-a.pdf> (accessed on 24 February 2021).

Xie, B., Goldberg, A., & Shi, L. (2022). A comprehensive evaluation of the potential binding poses of fentanyl and its analogs at the  $\mu$ -opioid receptor. *Computational and structural biotechnology journal*, 20, 2309–2321. <https://doi.org/10.1016/j.csbj.2022.05.013>

Yeadon, M., Kitchen, I., 1988. Comparative binding of  $\mu$  and  $\delta$  selective ligands in whole brain and pons/medulla homogenates from rat: Affinity profiles of fentanyl derivatives. *Neuropharmacology* 27, 345–348. [https://doi.org/10.1016/0028-3908\(88\)90141-4](https://doi.org/10.1016/0028-3908(88)90141-4)

Ylilauri, M., Pentikäinen, O.T., 2013. MMGBSA as a tool to understand the binding affinities of filamin-peptide interactions. *J. Chem. Inf. Model* 53(10):2626-33. doi: 10.1021/ci4002475

Yoshida, Y., Koide, S., Hirose, N., Takada, K., Tomiyama, K., Koshikawa, N., Cools, A.R., 1999. Fentanyl increases dopamine release in rat nucleus accumbens: Involvement of mesolimbic MU- and delta-2-opioid receptors. *Neuroscience* 92, 1357–1365. [https://doi.org/10.1016/S0306-4522\(99\)00046-9](https://doi.org/10.1016/S0306-4522(99)00046-9)

Zádor, F., Balogh, M., Váradi, A., Zádori, Z.S., Király, K., Szűcs, E., Varga, B., Lázár, B., Hosztafi, S., Riba, P., Benyhe, S., Fürst, S., Al-Khrasani, M., 2017. 14-O-Methylmorphine: A Novel Selective Mu-Opioid Receptor Agonist with High Efficacy and Affinity. *Eur. J. Pharmacol.* 814, 264–273. <https://doi.org/10.1016/j.ejphar.2017.08.034>

## Figure legends

**Figure 1. Chemical structures of isotonitazene (ITZ) metonitazene (MTZ), piperidylthiambutene (PTB) and fentanyl.**

**Figure 2. Concentration-response curves of compound-stimulated [ $^{35}$ S]GTP $\gamma$ S (A) and [ $^3$ H]DAMGO binding (B) to cortical rat membranes.** A: Rat cortical membranes were incubated with various concentrations of ITZ (magenta triangles), MTZ (blue squares), fentanyl (red inverted triangles), PTB (green diamonds) and DAMGO (black circles), as described in Material and Methods. Data are expressed as mean percentage of basal values of GTP $\gamma$ S binding  $\pm$  SEM of at least three independent experiments. B: Displacement curves of [ $^3$ H]DAMGO by ITZ, MTZ, fentanyl, PTB and DAMGO in rat cortical membranes. Data are expressed as means  $\pm$  SEM of at least three independent experiments, each performed in triplicate. The calculation of IC<sub>50</sub> was performed by non-linear curve fitting of the concentration effect curves using GraphPad Prism 8 software. The F-test was used to determine the best approximation of a non-linear curve fit to one or two site models ( $p < 0.005$ ). IC<sub>50</sub> values were converted to Ki values by means of the Cheng and Prusoff equation (Cheng and Pursoff, 1973). The parameters describing the different curves are given in Table 1 (The reader is referred to the web version of this article for interpretation of the color references in this figure legend.)  
Abbreviations: ITZ, isotonitazene; MTZ, metonitazene; PTB, piperidylthiambutene

**Figure 3. Concentration-response curves of agonist-stimulated [ $^{35}$ S]GTP $\gamma$ S (A) and [ $^3$ H]DAMGO binding (B) to CHO-MOR cell membranes.** A: Data represent means  $\pm$  SEM of three independent experiments, each performed in triplicate. IC<sub>50</sub> values were converted to Ki values by means of the Cheng and Prusoff equation (Cheng and Pursoff, 1973). K<sub>d</sub> and B<sub>max</sub> values for [ $^3$ H]DAMGO in CHO-MOR membranes are 1.93 nM  $\pm$  0.47 and 2.02  $\pm$  0.35 pmol/mg of protein. The parameters describing the different curves are given in Table 2. (The reader is referred to the web version of this

article for interpretation of the color references in this figure legend). Abbreviations: ITZ, isotonitazene; MTZ, metonitazene; PTB, piperidylthiambutene

**Figure 4. Dose-response curves of hot plate latency after ITZ, fentanyl, and morphine intravenous administration.** Results are shown as mean  $\pm$  SEM of the seconds (s) of hind paw or withdrawal during the hot plate test. The arrow indicates the i.v. injection of isotonitazene (ITZ), fentanyl, morphine, and respective vehicle. Panel A: ITZ (0.5-4  $\mu$ g/kg; variation of blue), (Vehicle, N=5; 0.5, N=5; 1, N=6; 2, N=6; 4, N=5). Panel B: fentanyl (1.25-10  $\mu$ g/kg; variation of green); (Vehicle-10, N=7 per group). Panel C: morphine (0.5-4 mg/kg; variation of red); (Vehicle, N=6; 0.5, N=5; 1, N=5; 2, N=6; 4, N=4); \*:  $p < 0.05$  vs vehicle (Two-way ANOVA; Tuckey's *post hoc* test).

(The reader is referred to the web version of this article for interpretation of the color references in this figure legend). Abbreviations: ITZ, isotonitazene.

**Figure 5. Mean effective dose ( $ED_{50}$ ) values after ITZ, fentanyl, and morphine intravenous administration.**  $ED_{50}$  values of ITZ (0.00156 mg/kg), fentanyl (0.00578 mg/kg), and morphine (2.35 mg/kg).

**Figure 6.**

**Dose-response curves of ITZ and MTZ intravenous administration on dopamine transmission in the NAc Shell.** Results are shown as mean  $\pm$  SEM of the changes in DA extracellular levels expressed as the percentage of basal values. The arrow indicates the i.v. injection of vehicle (black diamonds), ITZ 0.001 (blue diamonds), ITZ 0.003 (green diamonds), ITZ 0.01 (orange diamonds), MTZ 0.001 (brown diamonds), MTZ 0.01 (purple diamonds), MTZ 0.03 (green diamonds). Panel A: solid symbol:  $p < 0.05$  vs basal value; \*:  $p < 0.05$  ITZ 0.01 vs vehicle; §:  $p < 0.05$  ITZ 0.01 vs 0.001; +:  $p < 0.05$  ITZ 0.01 vs 0.003; (Vehicle, N=3; 0.001, N=4; 0.003, N=6; 0.01, N=7). Panel B: solid symbol:  $p < 0.05$  vs basal value; \*:  $p < 0.05$  MTZ 0.03 vs vehicle; §:  $p < 0.05$  MTZ 0.03 vs 0.001; (Vehicle,

N=3; 0.001, N=4; 0.03, N=8; 0.01, N=7); (Two-way ANOVA; Tuckey's *post hoc* test). (The reader is referred to the web version of this article for interpretation of the color references in this figure legend).

**Figure 7. Comparison of the effects of morphine, fentanyl, ITZ, and MTZ on DA transmission in the NAc Shell.** Results are shown as mean  $\pm$  SEM of the changes in DA extracellular levels expressed as the percentage of basal values. The arrow indicates the i.v. injection of vehicle (black circles), morphine (red squares), fentanyl (blue triangles), ITZ (orange diamonds) or MTZ (green diamonds), solid symbol:  $p < 0.05$  vs basal value; \*:  $p < 0.05$  ITZ vs vehicle; §:  $p < 0.05$  morphine vs vehicle; +:  $p < 0.05$  MTZ vs vehicle; °:  $p < 0.05$  ITZ vs MTZ; #:  $p < 0.05$  ITZ vs fentanyl; (Two-way ANOVA; Tuckey's *post hoc* test); (Vehicle, N=3; Morphine, N=4; Fentanyl, N=4; ITZ, N=7; MTZ, N=8). (The reader is referred to the web version of this article for interpretation of the color references in this figure legend). Abbreviations: ITZ, isotonitazene; MTZ, metonitazene.

**Figure 8. Sedation rating 10 min after morphine, ITZ, and MTZ intravenous administration.** Results are shown as mean  $\pm$  SEM of the score of the sedation rating. \*:  $p < 0.005$  vs vehicle; \*\*\*:  $p < 0.0001$  vs vehicle; #:  $p < 0.0001$  vs MTZ; (One-way ANOVA; Tuckey's *post hoc* test); (Vehicle, N=5; MTZ, N=6 Morphine, N=5; ITZ, N=6). Each empty dot represents the value of single animal (The reader is referred to the web version of this article for interpretation of the color references in this figure legend). Abbreviations: ITZ, isotonitazene; MTZ, metonitazene.

**Figure 9. Time-course of sedation rating after morphine, ITZ, and MTZ intravenous administration.** Results are shown as mean  $\pm$  SEM of the score of the sedation rating. Differences are referred to the respective time-points as follows: \*:  $p < 0.05$  vs ITZ 0.01; +:  $p < 0.001$  vs MTZ 0.03; (Two-way ANOVA; Tuckey's *post hoc* test); (Morphine, N=4; Vehicle-ITZ N=4; Vehicle-MTZ, N=4; ITZ, N=7; MTZ, N=8). ). Each empty dot represents the value of single animal (The

reader is referred to the web version of this article for interpretation of the color references in this figure legend). Abbreviations: ITZ, isotonitazene; MTZ, metonitazene.

**Figure 10. Electrostatic interactions within the binding site which are represented by dashed lines.**

ITZ and MTZ: electrostatic interaction between the nitro group and Lys 303 (K303), His 54 (H54) and Trp 318 (W318). PTB: aromatic contacts with His297 (H297) and Tyr 326 (Y326). Fentanyl: water bridge between Tyr 148 (Y148) and amidic carbonyl oxygen and aromatic interaction Tyr 326 (Y326). (The reader is referred to the web version of this article for interpretation of the color references in this figure legend). Abbreviations: ITZ, isotonitazene; MTZ, metonitazene; PTB, piperidylthiambutene

**Figure 11. Hydrophobic interactions within the binding site.** Hydrophobic interactions between ligand (green) and receptor binding pocket (grey dots). (The reader is referred to the web version of this article for interpretation of the color references in this figure legend). Abbreviations: ITZ, isotonitazene; MTZ, metonitazene; PTB, piperidylthiambutene

**Figure 12. Electrostatic surface distribution of MOR in the active form bound to ITZ and MTZ.** (A) represents the electrostatic surface of ITZ (colored cloud). The red circle shows the electrostatic area of the isopropoxy extra portion compared to (B) the electrostatic surface of MTZ. Comparison of the structural rearrangements for MOR His54 (C) induced by ITZ (1) and MTZ (2), respectively. The shift range is of 123.3° degrees.

**Figure 13. Structural rearrangements during receptor activation.**(A) Cluster of IFD molecular models on MOR inactive form. The structural rearrangements of the TMH3 D147, M151 and N150 residues, crucial for receptor activation, when bound to the crystallographic antagonist BF0 (fuchsia), the crystallographic agonist BU72 (green), ITZ (cyan) and MTZ (orange). (B) IFD molecular models

on MOR active form representing the structural rearrangements of the TMH3 D147, M151 and I155 residues, when bound to ITZ (cyan) and MTZ (orange). The M151 induced flip by ITZ (yellow) and MTZ (purple) is indicated with a circle.



Table 1

Binding affinity, potency and efficacy for stimulation of [<sup>35</sup>S]GTP $\gamma$ S binding in rat cortical membranes.

COMPOUNDS	MOR Ki (nM)	EC <sub>50</sub> (nM)	GTP $\gamma$ S BINDING	
			E <sub>max</sub> (%) relative to basal	DAMGO
DAMGO	0.23 ± 0.01	310 ± 51.5	144 ± 6.9	100
ITZ	0.06 ± 0.01*#§	0.99 ± 0.1***+	131 ± 2.9	91 ± 2.0
MTZ	0.22 ± 0.01 <sup>§</sup>	19.1 ± 1.8***+	131 ± 2.4	91 ± 1.6
FENTANYL	1.09 ± 0.06***	124 ± 17.7***+	127 ± 2.6	88 ± 1.8
PTB	2.75 ± 0.03***	587.0 ± 46.5*** <sup>§</sup>	141 ± 4.8	97 ± 3.2

Data are the means ± SEM of at least three experiments, each performed in triplicate. The calculation of IC<sub>50</sub> was performed by non-linear curve fitting of the concentration effect curves using GraphPad Prism 8 software (GraphPad Prism, RRID:[SCR\\_002798](#)). IC<sub>50</sub> values were converted to Ki values by means of the Cheng and Prusoff equation (Cheng and Pursoff, 1973). Compound- mediated [<sup>35</sup>S]GTP $\gamma$ S binding data represent percentage of stimulation over basal values (set as 100%). E<sub>max</sub> and EC<sub>50</sub> were determined by nonlinear regression curve fit (GraphPad Prism 8 software). One way ANOVA: Ki: F<sub>(4,10)</sub> = 1288, P<0.0001; EC<sub>50</sub>: F<sub>(4,13)</sub> = 65.00 P < 0.0001; E<sub>max</sub>: F<sub>(4,13)</sub> P=0.066; \*p < 0.05, \*\*p < 0.01 and \*\*\*p < 0.001 compared to DAMGO; # p < 0.05 compared to metonitazene; § p < 0.001 compared to fentanyl; and + p < 0.001 compared to piperidylthiambutene; (Dunnett's test). Abbreviations: ITZ, isotonitazene; MTZ, metonitazene; PTB, piperidylthiambutene

Table 2

Binding affinity, potency and efficacy for stimulation of [<sup>35</sup>S]GTPγS binding in CHO-MOR membranes.

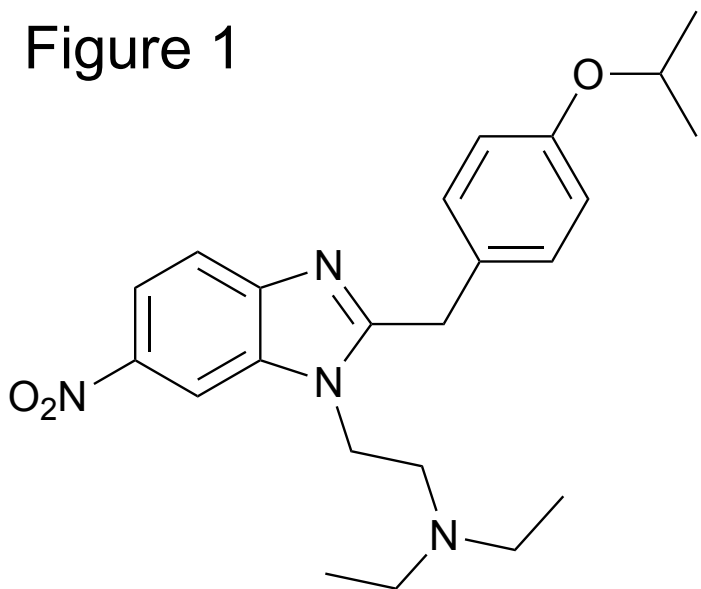
COMPOUNDS	GTPγS BINDING			
	MOR	EC <sub>50</sub> (nM)	E <sub>max</sub> (%) relative to	
	Ki (nM)		basal	DAMGO
DAMGO	1.22 ± 0.05	69.58 ± 12.99	426 ± 73	100
ITZ	0.05 ± 0.01**	0.71 ± 0.15**+	435 ± 46	102 ± 10.8
MTZ	0.23 ± 0.04*	10.04 ± 1.13*+	422 ± 29	99 ± 6.6
PTB	3.72 ± 0.34***	122.7 ± 14.84*	408 ± 29	96 ± 6.8

Data are the means ± SEM of at least three experiments, each performed in triplicate. The calculation of IC<sub>50</sub> was performed by non-linear curve fitting of the concentration effect curves using GraphPad Prism 8 software (GraphPad Prism, RRID:[SCR\\_002798](#)). IC<sub>50</sub> values were converted to Ki values by means of the Cheng and Prusoff equation (Cheng and Pursoff, 1973). Compound- mediated [<sup>35</sup>S]GTPγS binding data represent percentage of stimulation over basal values (set as 100%). E<sub>max</sub> and EC<sub>50</sub> were determined by nonlinear regression curve fit (GraphPad Prism 8 software). One way ANOVA: Ki: F<sub>(3,8)</sub> = 94.22, P < 0.0001; EC<sub>50</sub>: F<sub>(3,8)</sub> = 33.10 P < 0.0001; E<sub>max</sub>: F<sub>(3,8)</sub> P = 0.052; \*p < 0.05, \*\*p < 0.01 and \*\*\*p < 0.001 compared to DAMGO; + p < 0.001 compared to piperidylthiambutene. (Dunnett's test). Abbreviations: ITZ, isotonitazene; MTZ, metonitazene; PTB, Piperidylthiambutene.

**Table 3.** Glide/XP, MM-GBSA, IFD, MD/pose scores for the crystallographic ligand BU72, ITZ, MTZ, PTB and Fentanyl, used as reference ligand.

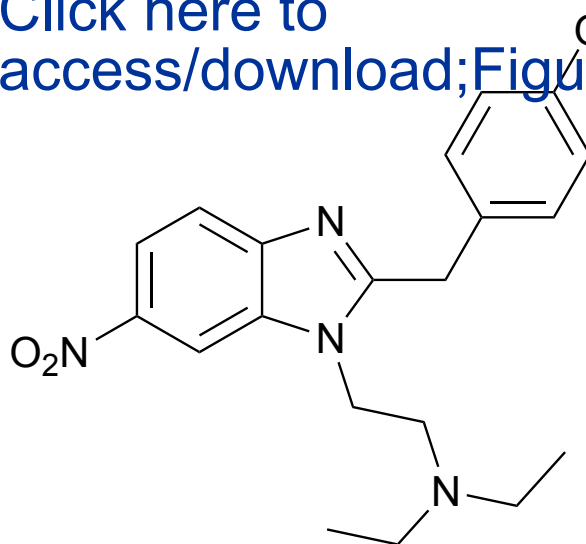
<b>COMPOUNDS</b>	<b>GLIDE/XP (Kcal/mol)</b>	<b>MM-GBSA (Kcal/mol)</b>	<b>IFD (Kcal/mol)</b>	<b>MD/PoseScore (Å)</b>
BU72	-9.908	-549.36	-116.76	-
ITZ	-6.867	-98.28	-547.76	1.355
MTZ	-6.544	-83.58	-547.17	1.356
FENTANYL	-6.355	-98.88	-545.94	1.509
PTB	-6.636	-80.77	-545.78	2.571

Figure 1

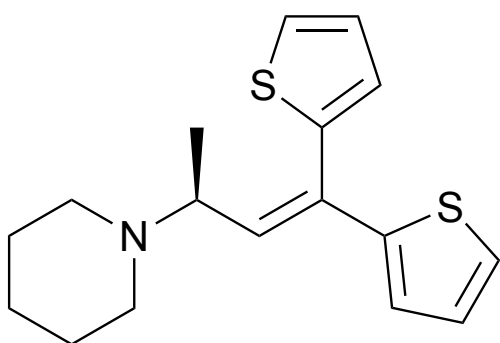


**ITZ**

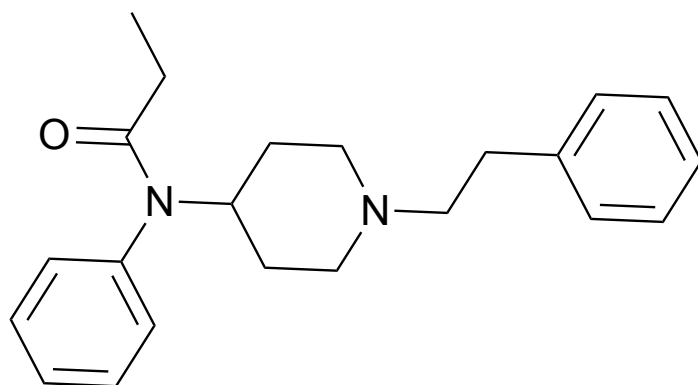
[Click here to access/download;Figure](#) 



**MTZ**



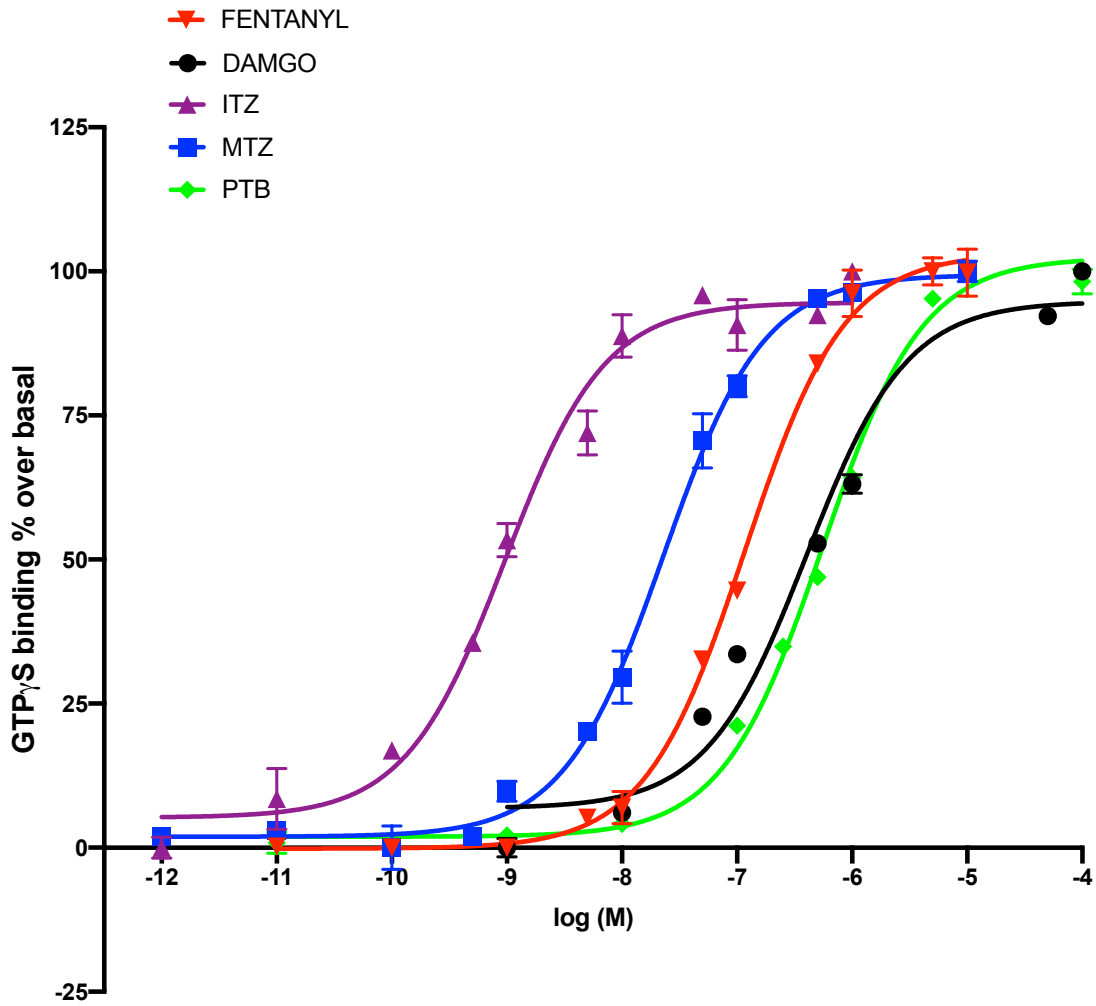
**PTB**



**Fentanyl**

Figure 2  
**A**

[Click here to access/download;Figure\(s\);Figure 2.pdf](#)



**B**

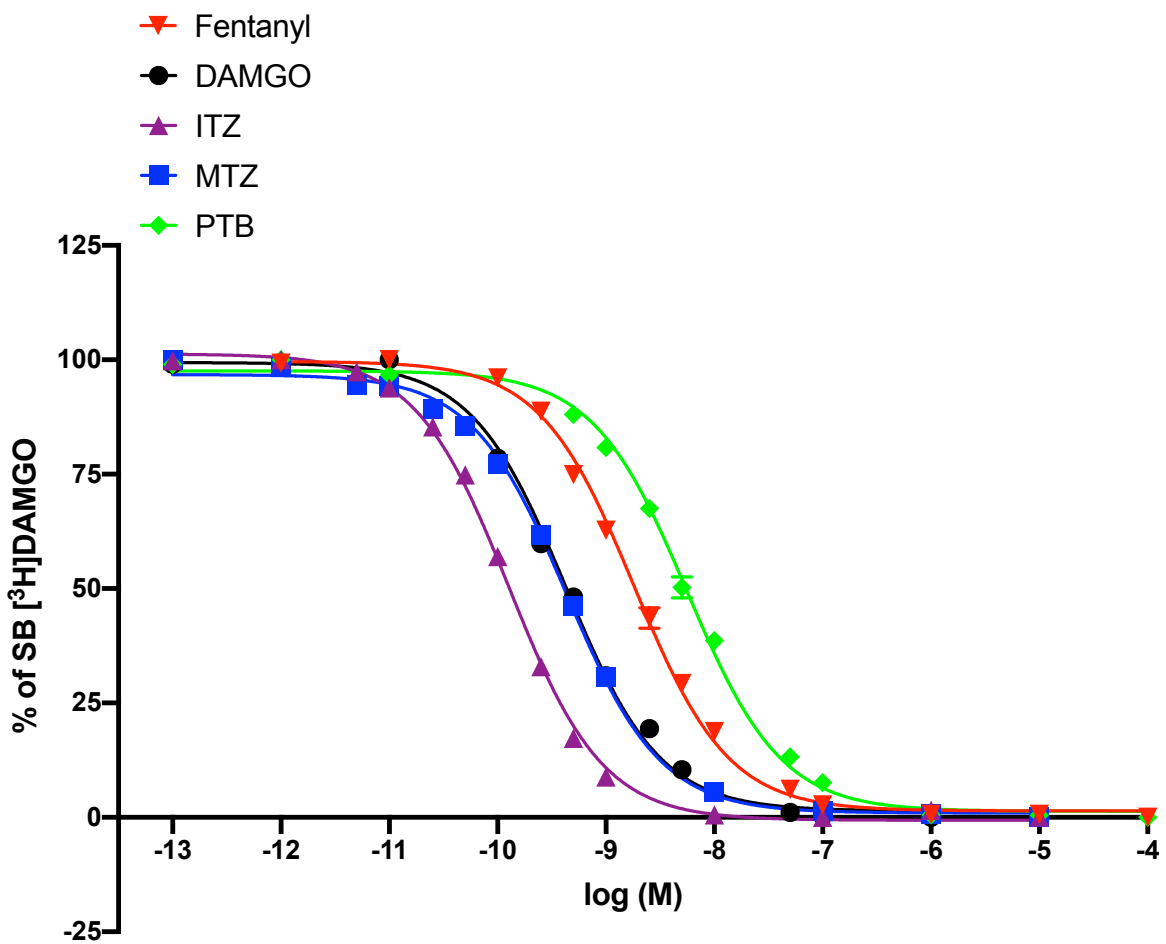
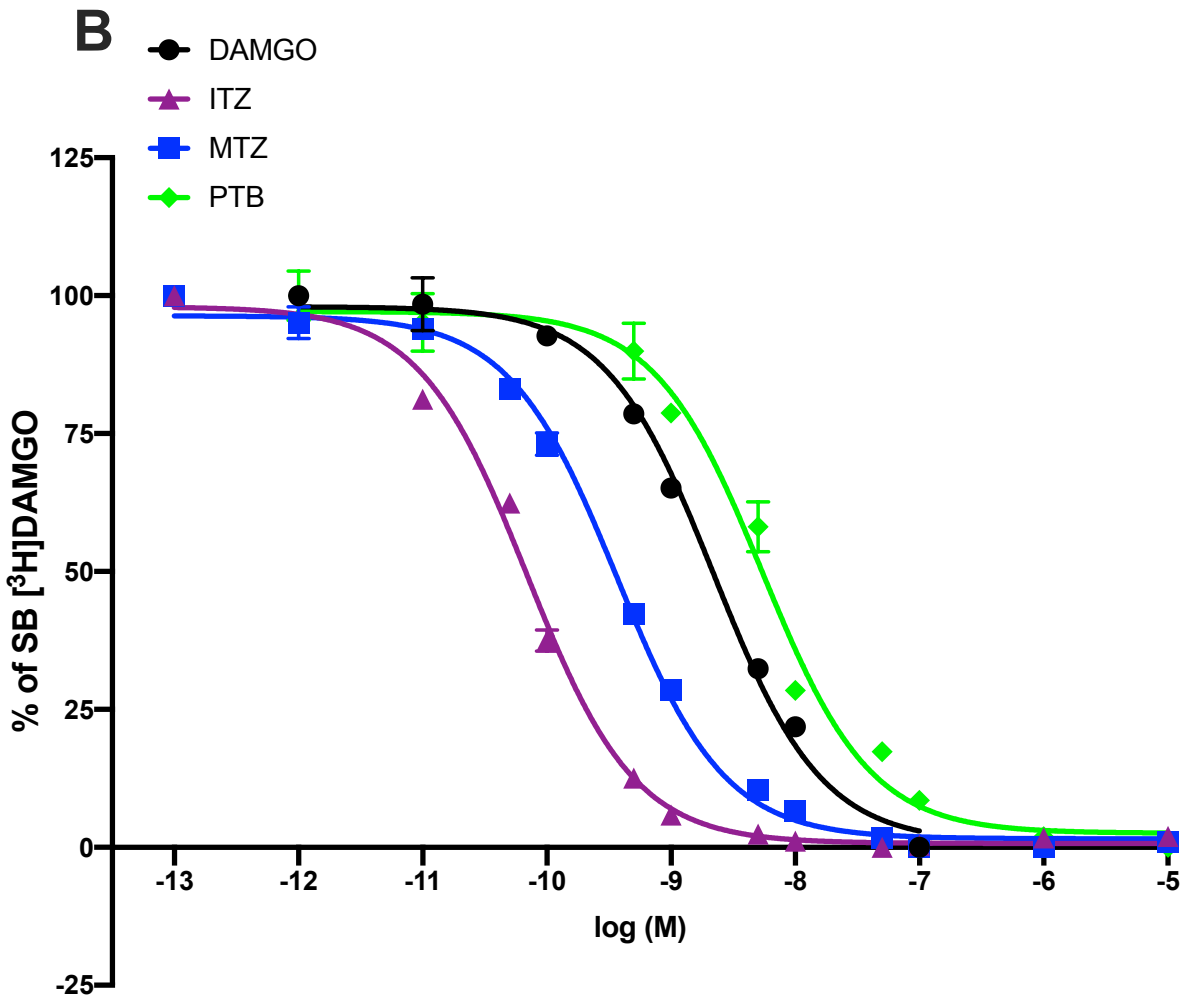
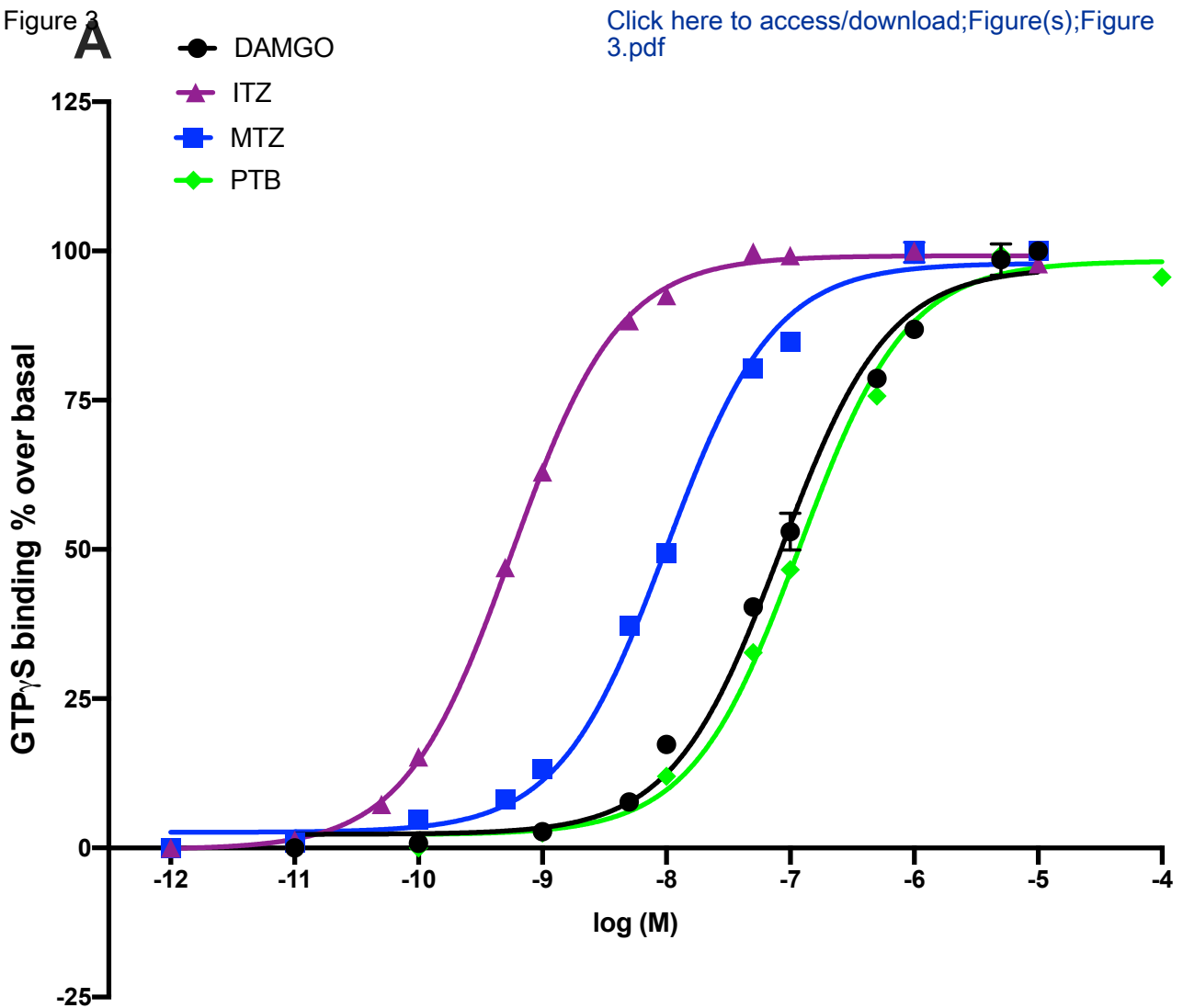
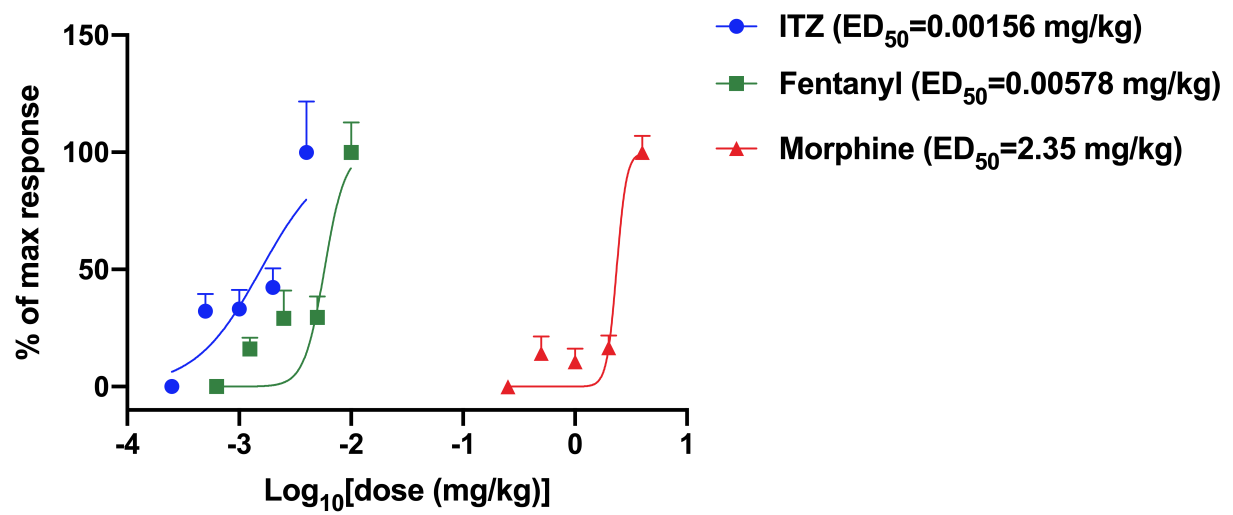


Figure 2

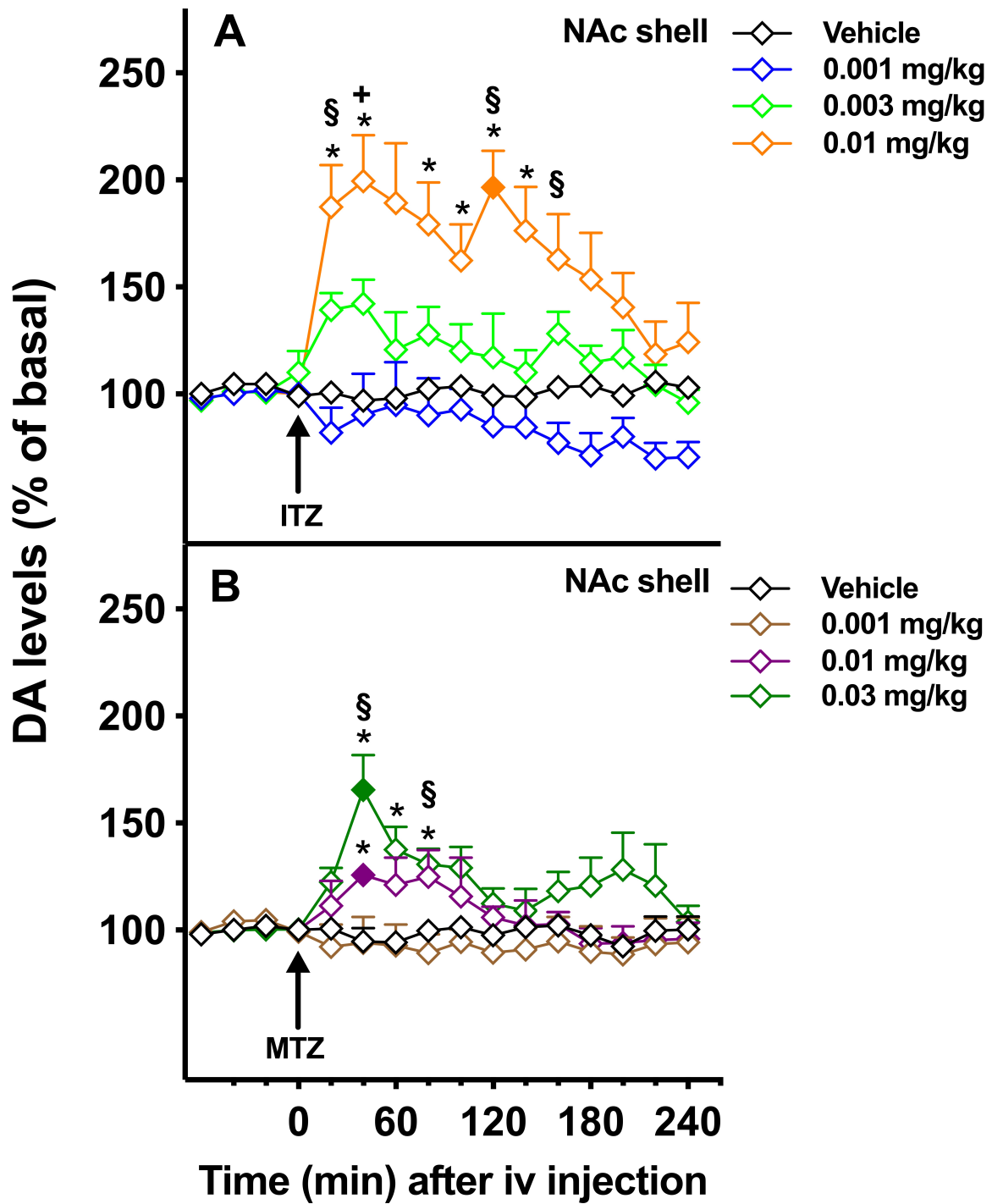
[Click here to access/download;Figure\(s\);Figure 3.pdf](#)

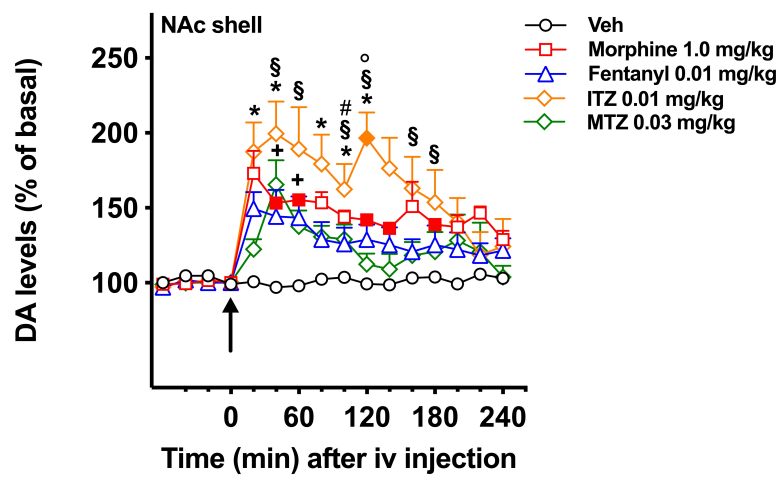


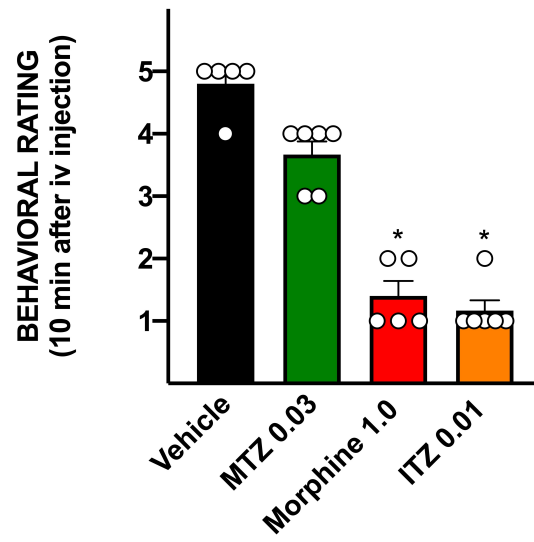


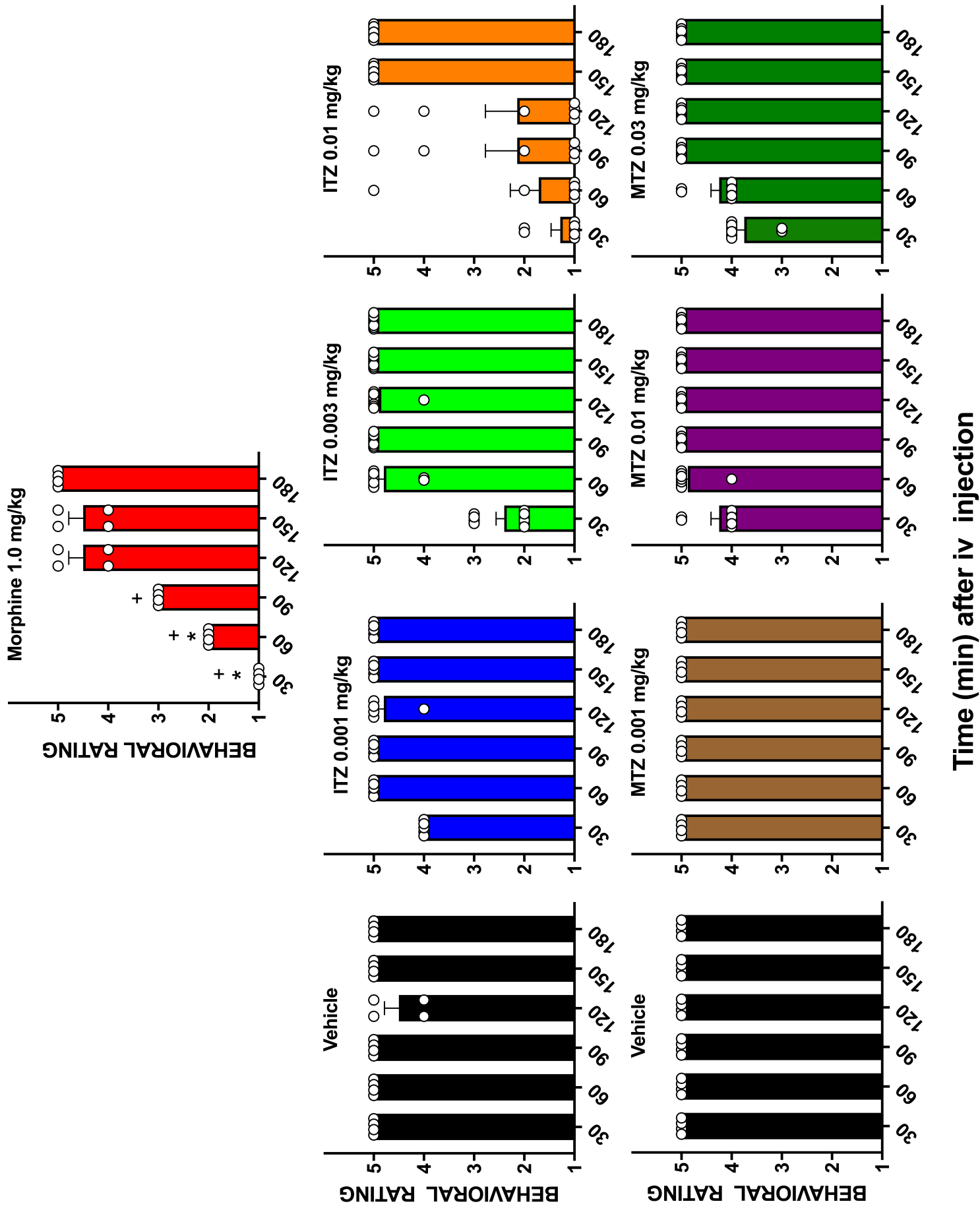




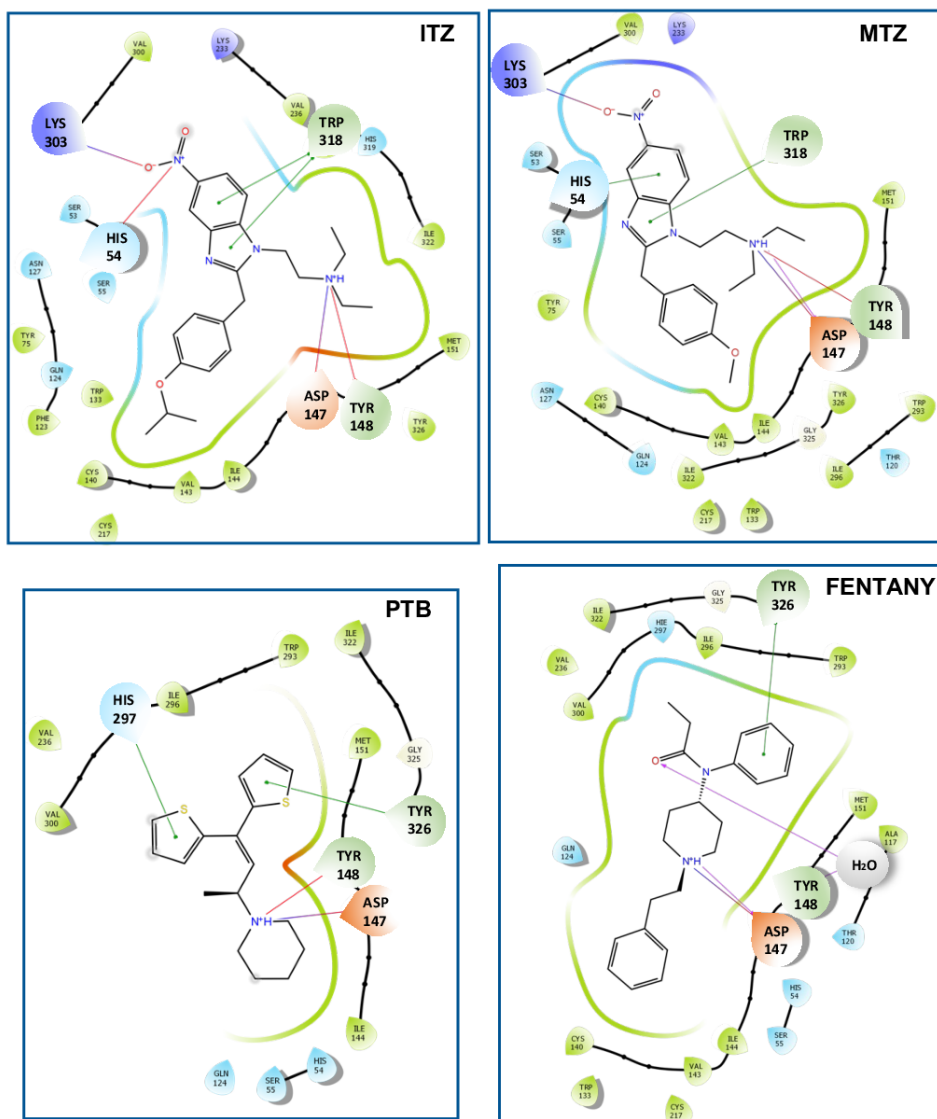






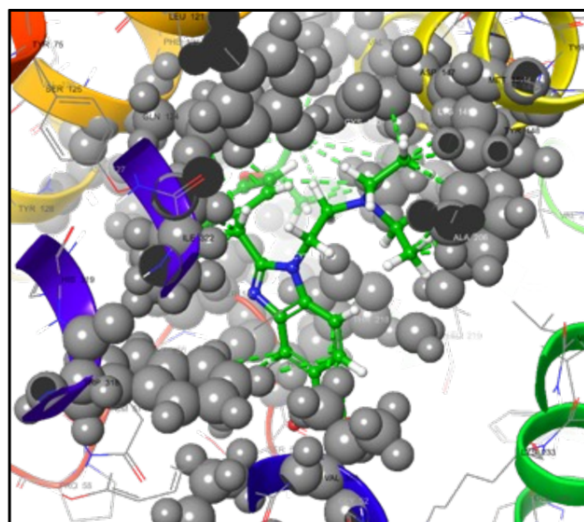


Time (min) after iv injection

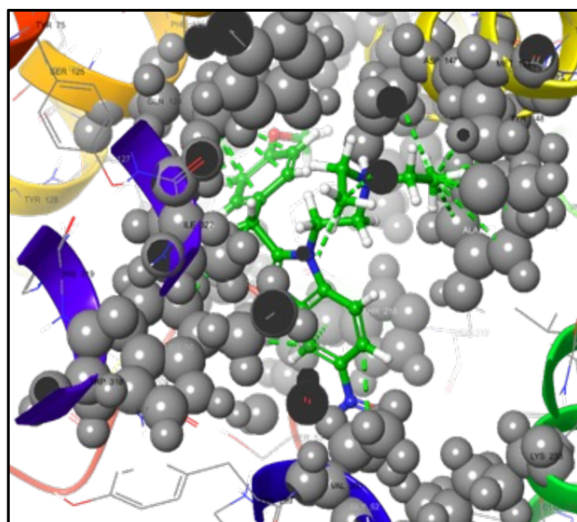


- |                    |                            |                    |                  |
|--------------------|----------------------------|--------------------|------------------|
| Charged (negative) | Polar                      | Distance           | Pi-cation        |
| Charged (positive) | Unspecified residue        | H-bond             | Salt bridge      |
| Glycine            | Water                      | Halogen bond       | Solvent exposure |
| Hydrophobic        | Hydration site             | Metal coordination |                  |
| Metal              | Hydration site (displaced) | Pi-Pi stacking     |                  |

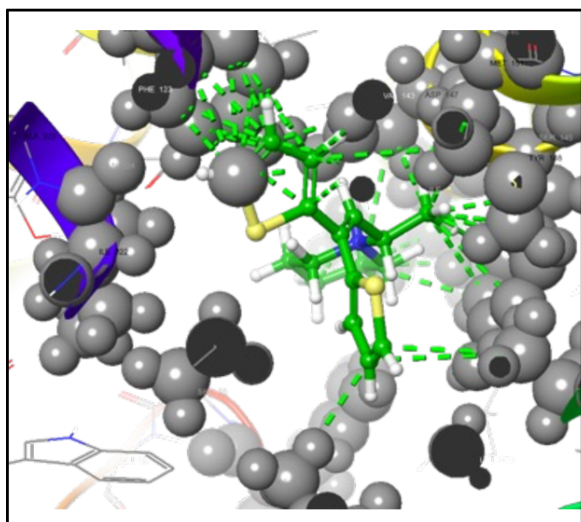
ITZ



MTZ



PTB



FENTANYL

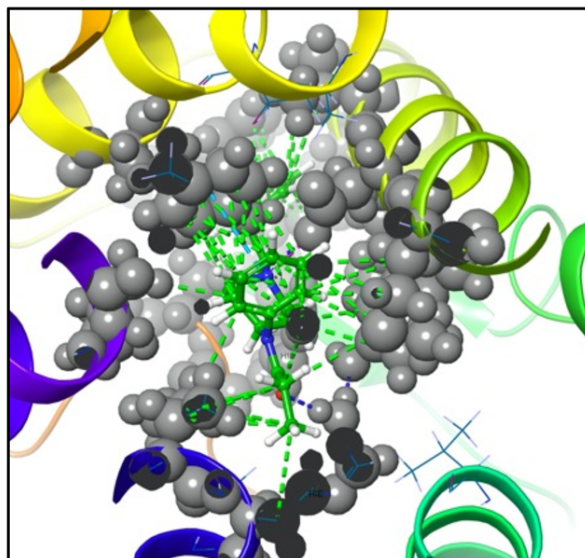
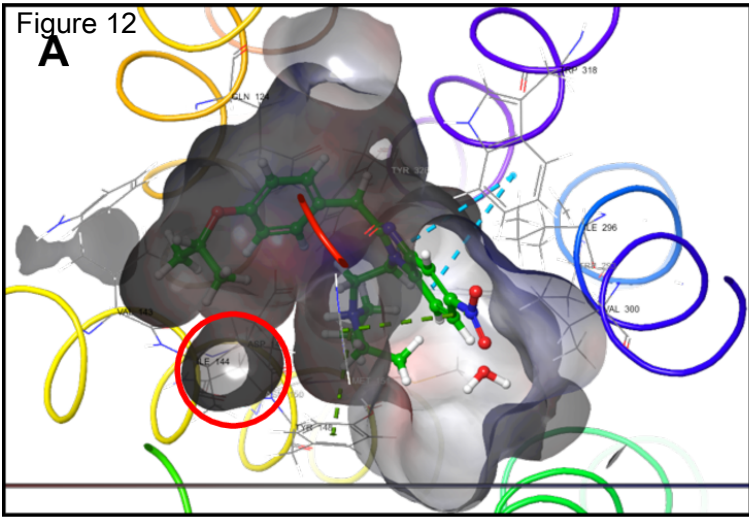


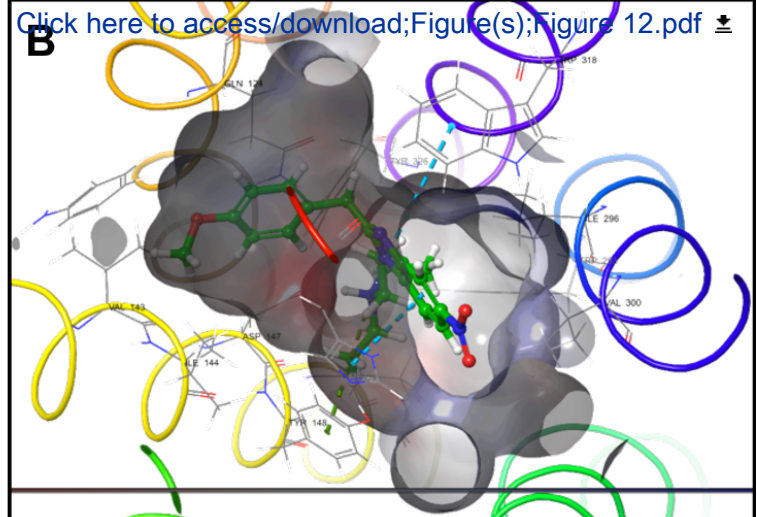
Figure 12

**A**



[Click here to access/download;Figure\(s\);Figure 12.pdf](#)

**B**



**C**

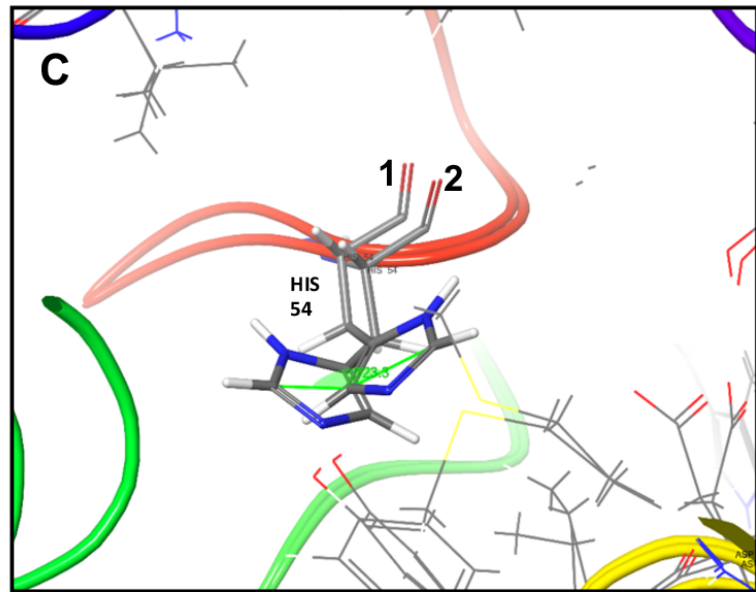
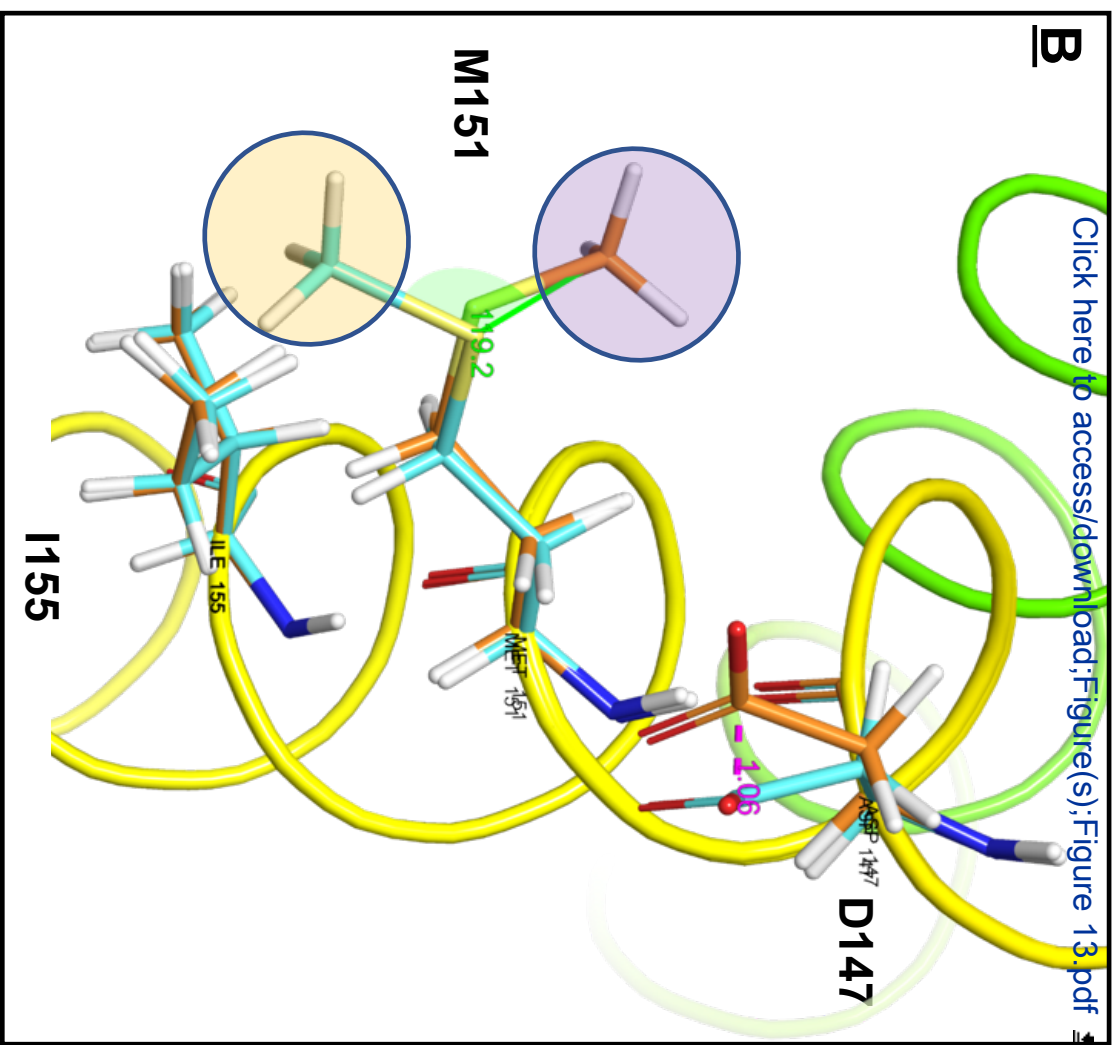
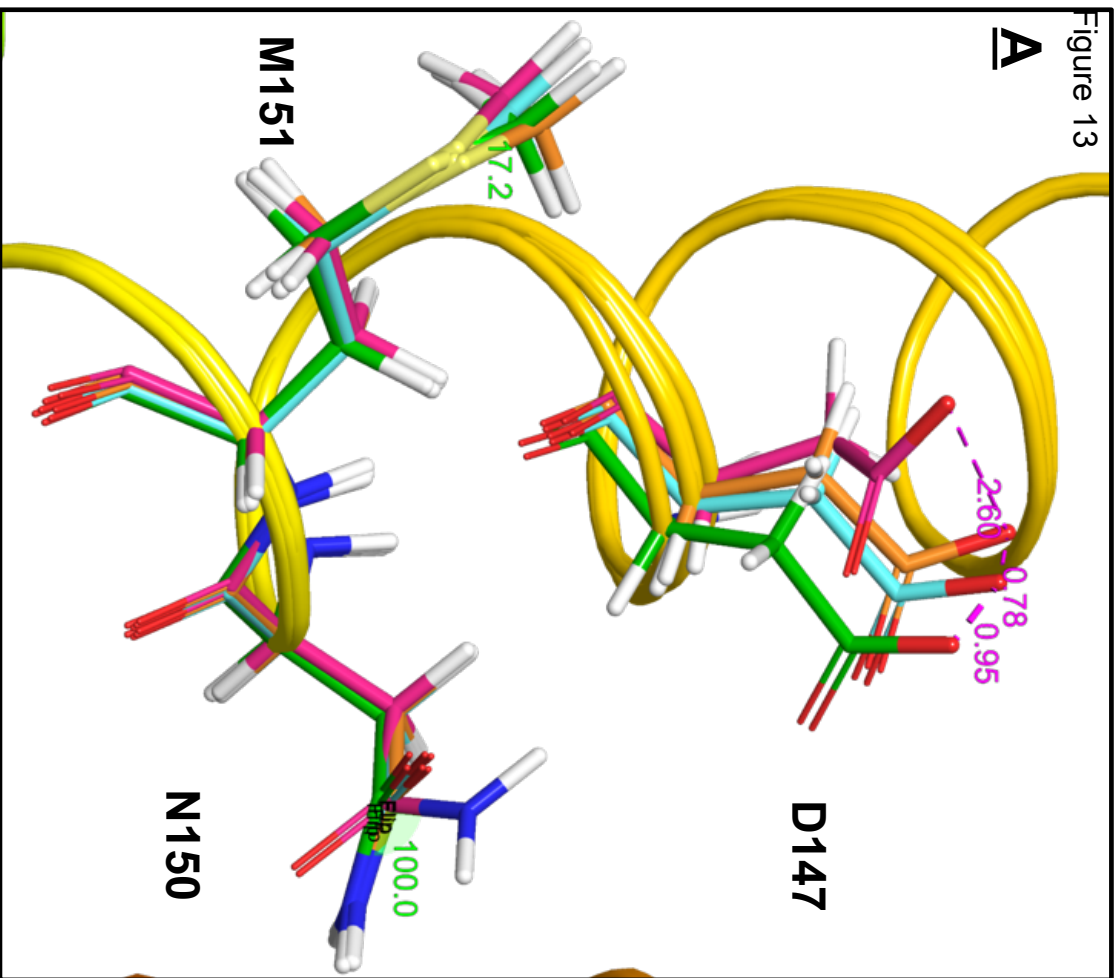



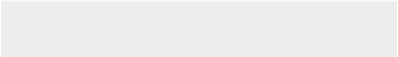

Figure 13





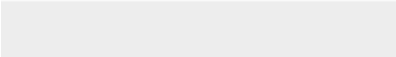




Click here to access/download  
**Supplementary Material**  
Suppl. Mat.docx



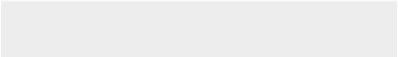



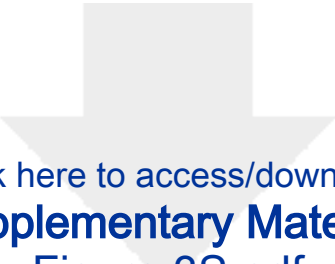
Click here to access/download  
**Supplementary Material**  
Figure 1S.pdf



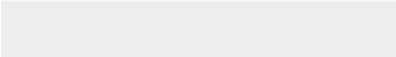



Click here to access/download  
**Supplementary Material**  
Figure 2S.pdf





Click here to access/download  
**Supplementary Material**  
Figure 3S.pdf



**CRedit authorship contribution statement**

**Maria Antonietta De Luca:** In vivo investigation, Formal Analysis, Conceptualization, Writing – original draft- review & editing. **Graziella Tocco:** Validation, In silico Investigation, formal analysis. **Rafaella Mostallino:** In vitro Investigation, Formal Analysis; **Antonio Laus:** In silico Investigation, Formal Analysis. **Francesca Caria:** In vivo Investigation. **Aurora Musa:** In vivo Investigation. **Nicholas Pintori:** Statistical analysis and graphical revision. **Marcos Ucha:** Behavioral evaluation. **Celia Poza:** Behavioral evaluation. **Emilio Ambrosio:** Validation, Behavioral evaluation, Formal Analysis. **Gaetano Di Chiara:** Conceptualization, Supervision, Writing – review & editing. **M Paola Castelli:** Conceptualization, In vitro Investigation, Writing – review & editing.